NTNU
Det skapende universitet

MPC for dual gradient borebrønnkontroll ved hjelp av en undervannspumpemodul og en topside strupeventil

Andreas Magnus

Master i teknisk kybernetikk og robotikk
Innlevert: juni 2014
Hovedveileder: Lars Imsland, ITK
Medveileder: Espen Hauge, Statoil
John-Morten Godhaven, Statoil

Norges teknisk-naturvitenskapelige universitet
Institutt for teknisk kybernetikk

NTNU

Faculty of Information Technology, Mathematics and Electrical Engineering
Department of Engineering Cybernetics

PROJECT DESCRIPTION SHEET

Name of the candidate: Andreas Magnus

Thesis title (Norwegian):

Thesis title (English): MPC for dual gradient drilling well control using a subsea mud pump and a topside choke

Background

Dual gradient drilling (DGD) is a relatively new method for drilling in deep-water and challenging reservoirs. The main features of DGD are the ability to quickly control the bottomhole pressure (BHP) by using the subsea pump module (SPM) to reduce the level in the riser. An incident such as gas influx, also called a gas kick, to the wellbore leads to a delicate operation where the pressure in the well must be controlled while gas is being circulated out of the well. At the same time the pressure in the well must be kept within the limits dictated by the formation. This project will focus on use of model predictive control (MPC) where the SPM, rig pump, and a choke are used to safely circulate a gas kick out of the well.

This project is given by Statoil ASA.

Work description

1. Do a literature survey on well control for managed pressure drilling, focusing on DGD, and describe the control problem.
2. Augment a provided Dymola model with the functionality needed for the control task.
3. Make base cases where manual control is used to circulate out the gas for comparison with results using automatic control.
4. Connect Dymola and Statoil's in-house MPC tool (SEPTIC) via OPC.
5. Use SEPTIC with dynamic models to efficiently circulate out gas of the annulus. Find the largest gas kick which safely can be circulated out of the well using MPC

Start date: 14. January, 2014 **Due date:** 10. June, 2014

Supervisor: Lars Imsland
Co-advisor(s): Espen Hauge and John-Morten Godhavn, Statoil

Trondheim, __14. January 2014_____

Lars Imsland
Supervisor

Address Sem Sælandsvei 5 NO-7491 Trondheim
Org.no. 974 767 880 E-mail: postmottak@itk.ntnu.no http://www.itk.ntnu.no
Location O.S. Bragstads plass 2D NO-7034 Trondheim
Phone + 47 73 59 43 76
Fax + 47 73 59 45 99
Phone: + 47 47 23 19 49

NORWEGIAN UNIVERSITY OF SCIENCE AND TECHNOLOGY

Abstract

Faculty of Information Technology, Mathematics and Electrical Engineering
Department of Engineering Cybernetics

MPC for dual gradient drilling well control using a subsea mud pump and a topside choke

by Andreas Magnus

This thesis investigates how well a linear MPC with dynamic models can control the bottom hole pressure (BHP) when a dual gradient system (DGD) is subjected to gas kicks. The MPC uses a rig pump, subsea pump module and a choke as manipulated variables (MV) to control the BHP, which is the only controlled variable (CV). The MPC models has been developed through experiments and describes step responses from each MV to the BHP. In addition gain scheduling and time constant adjustment is implemented to take the varying gain into account as well as the altered time constant due to kick. A simple estimator integrating the difference of mud influx and outflow has been implemented to make this possible. The MPC has been tuned to utilize the SPM as much as possible to avoid unnecessary power consumption and wear.

The MPC managed to safely ventilate out gas kicks as large as 32 barrels at bottom hole conditions while maintaining the BHP within a ± 2.5 bar margin. This was considerably better than the reference case which featured a simple PI controller that manipulated the choke only. However, it must be mentioned that this system utilizes a multiphase meter to find out when the SPM should be set in idle. This is clearly a disadvantage since a multiphase meter will represent a significant cost for the entire project.

NORGES TEKNISK-NATURVITENSKAPLIGE UNIVERSITET

Sammendrag

Fakultet for informasjonsteknologi, matematikk og elektroteknikk
Institutt for teknisk kybernetikk

MPC for dual gradient drilling well control using a subsea mud pump and a topside choke

av Andreas Magnus

Denne avhandlingen undersøker hvor godt en lineær MPC med dynamiske modeller kan kontrollere bunnhullstrykket (BHP) når et "dual-gradient" boresystem (DGD) utsettes for gass-kick. MPC-en anvender en riggpumpe, undervannspumpemodul (SPM) og en strupeventil som manipulerte variabler (MV) for å styre BHP, som er den eneste regulerte variabelen (CV). MPC modellene har blitt utviklet gjennom eksperimenter og beskriver sprangresponser fra hver MV til BHP. I tillegg er det implementert dynamisk forsterkning og dynamisk justering av tidskonstant for å ta høyde for systemets varierende forsterkning, så vel som den endrede tidskonstanten på grunn av gassen i systemet. En enkel estimator av gass-kick-volumet har blitt implementert ved å integrere forskjellen av borevæske som strømmer inn og ut for å gjøre dette mulig. MPC-en er blitt innstilt til å utnytte SPM-en så mye som mulig for å unngå unødvendig kraftforbruk og slitasje.

MPC-en klarte å ventilere ut gass-kick så store som 32 fat, målt ved bunnhullsforhold, og samtidig opprettholde BHP innenfor en margin på ± 2,5 bar. Dette var betydelig bedre enn referanse-systemet som brukte en enkel PI-regulator til a styre strupeventilen. Det må imidlertid nevnes at dette systemet benytter en flerfasemåler for å finne ut når SPM-en bør spinnes ned til lavt turtall. Dette er helt klart en ulempe ettersom en flerfasemåler vil utgjøre en betydelig kostnad for hele prosjektet.

Preface

This master thesis has been given as a follow up of my specialization project conducted prior to this work. The research was carried out in my 10^{th} and final semester of my studies in engineering cybernetics at NTNU in cooperation with Statoil.

The project's supervisor has been prof. Lars S. Imsland and co-advisers has been Ph.D. Espen Hauge and Prof. II John-Morten Godhavn at Statoil.

I would like to thank all my advisor's for great help and guidance through this spring. In addition I would like to thank Morten Fredriksen who has given me great help and insight in the MPC-tool SEPTIC.

Trondheim, June 2014

_____

Andreas Magnus

Contents

List of Figures

Abbreviations

MPD	**M**anaged **P**ressure **D**rilling
DGD	**D**ual **G**radient **D**rilling
MRL	**M**ud **R**eturn **L**ine
BOP	**B**low-**O**ut **P**reventer
BHP	**B**ottom-**H**ole **P**ressure
SPM	**S**ubsea **P**ump **M**odule
PI	**P**roportional **I**ntegral
SPP	**S**tand **P**ipe **P**ressure
MPC	**M**odel **P**redictive **C**ontrol
lpm	**l**itre **p**er **m**inute
rpm	**r**evolutions **p**er **m**inute
SEPTIC	**S**tatoil **E**stimation & **P**rediction **T**ool for **I**dentification & **C**ontrol
OPC	**O**le for **P**rocess **C**ontrol
CV	**C**ontrolled **V**ariable
MV	**M**anipulated **V**ariable

Chapter 1

Introduction

Up until recent years offshore drilling for oil has been fairly easy requiring only very basic control systems. While the well is being drilled it is filled up with special liquid called drilling mud which serves two purposes. Firstly, it provides a pressure increase down the well which is necessary to keep the well from collapsing as the ambient pressure is increasing with depth. Secondly, it allows the cuttings to be circulated out of the well as the drilling bit works its way down. This is done by pumping mud through the drill string out by the drilling bit and then let it flow back through the annular room in the well called the annulus. In this simple setup the bottom hole pressure (BHP) is controlled only at certain intervals at which points the density of the drilling mud is changed.

As the oil wells becomes more difficult to drill due to larger water depth and more unstable ground, more sophisticated control schemes are needed to overcome the new challenging environments. To accommodate these challenges managed pressure drilling (MPD) emerged as the solution mostly used in the industry. The variations of MPD are many and one of the earliest and simplest configurations was to use a lighter drilling mud and close off the system at the top of the riser with a choke which compensates the BHP for the lighter mud density [1]. This configuration allows the BHP to be controlled fast and accurate by manipulating the choke opening.

The configuration used in this thesis is a fairly new method called dual gradient drilling (DGD) which utilizes two drilling muds with different densities creating two pressure gradients in the system, hence the name. Above the seabed a mud with density equal to seawater is used and down hole a denser mud is used to better fit the ambient pressure profile in the well. To keep the two muds from getting mixed the dense well-mud is passed though a separate pipe called mud return line (MRL) up to the platform. A subsea pump module (SPM) is placed at the bottom of the MRL to compensate for the denser mud relative to the mud in the riser. A more comprehensive description of system can be found in Chapter 2.

All these drilling techniques has been subjected to extensive research in recent years using many different controllers. The configurations span from using just a simple PI controller to adjust the choke, to the more advanced model predictive controller (MPC) utilizing all the actuators.

1.1 Problem description

In this thesis the DGD system will be controlled by a linear MPC which manipulates the rig pump flow, the SPM and a choke placed at the end of the MRL. A very similar configuration has been researched in [2] were the DGD system was controlled with and without MPC. However, unlike this research which dealt with normal operation and compensation of vertical drill string movement, this thesis will address the difficulties which arises when a gas kick is propagating up from the bottom towards the platform.

The drilling system used in this work is a well proven model for the drilling facilities at Troll modelled in Modelica by Statoil. It is controlled by Statoil's in-house MPC-tool SEPTIC via the OPC protocol. In addition, a reference case using only a PI controller to operate the choke has been made for comparison.

An attempt to explore the advantages of using MPC as described above was done in my specialization project the fall of 2013. Although it was clear that the MPC

increased the systems capabilities regarding out-circulation of gas, it was obviously not applicable in a real system as it exhibited violent oscillations in both BHP and choke opening. It was also identified that the sudden head loss and gain in the SPM caused pressure spikes which the MPC handled badly.

In order to fix these problems a new attempt is carried out in this thesis were the models used by the MPC have varying gain and time constant. In addition a new routine is employed to spin down the SPM in order to avoid the sudden pressure spikes at gas entry and exit of the SPM.

Chapter 2

Drilling

2.1 Conventional drilling

When drilling rig is starting on a new well a blowout preventor (BOP) is placed on the seabed and a large pipe called a riser is lowered down from the rig and attached to the BOP. The riser which now connects the rig with the BOP is then filled with liquid called drilling mud which is denser than seawater and therefore forces the seawater inside out through the top of the riser. Next, a drill string with a drill bit attached to the end is lowered down inside the riser. The drill string is hollow allowing mud to flow down inside the string and out of the drill bit into the riser. At the top of the drill string a rig pump pumps mud through the system making it possible to circulate out cuttings from the bottom. The mud together with the cuttings exits the system at the top of the riser and is processed on the rig before being pumped down again.

When the drill bit has reached a certain depth beneath the seabed the well is reinforced with steel casings cemented to wall before continuing with a denser drilling mud in order to keep the BHP within the calculated pressure margins. Depending on how deep the well needs to be this is repeated several times.

2.2 Pore and fracture pressure

When drilling a well it is important to keep the BHP within certain boundaries given by the masses enclosing the well. These masses can consist different kind of rock and soils which can more or less stable. If for instance the BHP drops below a threshold known as the pore pressure, the walls of the well will start leaking gas, oil or other unstable formations into the well. If on the other hand the BHP rises above a threshold called fracture pressure, expensive mud will leak out of the well into the surroundings and it will also make it more difficult for the bit to drill into the formations.

If the BHP drops below a even lower threshold than the pore pressure called the collapse pressure, the well will collapse on it self which in turn can cause the drill string to get stuck. In such events the only solution is to abandon the well and all the equipment inside it and start over at a different location.

The pore and fracture pressure may vary in a piecewise linear way down through the well, see Figure 2.1. At the vertex between section 1 and 2 it is evident that its impossible to continue with the current mud density. At this point section 1 of the well gets reinforced with a new casing before continuing with a denser mud in section 2.

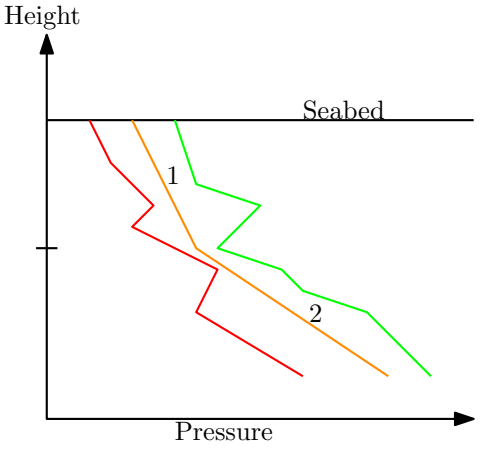

FIGURE 2.1: The pressure window is between the red and green curve and the mud pressure in orange.

Before the drilling can start geologists will gather information about the formations in that area and calculate estimates of the applicable pressure window. As the drilling progresses the estimates are updated in order to keep the estimates within reasonable margin of error. These estimates will always have some uncertainty and a set point in the middle

of the thresholds is computed in order to minimize the risk of violating the actual limits. It is this set point that will be the target for the BHP when the system is subjected to control later on.

In this thesis the estimates is assumed to be known in all simulations. Further, since the well isn't expanded during the simulations, the thresholds are constant throughout the simulations.

2.3 Gas kick

As mentioned in the previous section the pore pressure never known, only estimated. This implies that there is a risk of gas influx if the estimate turned out to be too low compared to the real pore pressure. These kind of gas influxes is known as kicks because it usually leads to a sudden pressure increase. However, as the gas propagates upwards in the system the pressure in the gas will drop causing it to expand leading to a less dense liquid column. As a result the BHP will drop depending on how much mud the gas displaces.

In addition to the lighter liquid column, the gas lift effect will contribute to lower the BHP as well[3]. As the gas rises to the drilling rig it will obtain a higher speed than the mud due to its buoyancy relative to the mud. However, due to friction between the gas and the mud, the gas will transfer some of its momentum to the mud. This relation is known as slip factor or slip ratio and is defined as the ratio between the velocities[4]. In the cited literature this ratio is defined inversely to definition used in the simulation software, Dymola, used in the thesis. Thus the version used here is the same as the one implemented in Dymola:

$$S = \frac{v_l}{v_g} \tag{2.1}$$

where S is the slip ratio, v_l is the velocity of the liquid and v_g is the velocity of the gas.

2.4 Managed pressure drilling

In order to maintain the BHP during the whole drilling operation additional pumps and chokes is applied to the drilling system. By adjusting pump speeds and choke openings it is possible to compensate for disturbances as soon as they are measured. Drilling systems which applies such actuators are known as managed pressure drilling (MPD) systems. At first, all these actuators was operated manually by the drilling crew, but due to the strong interconnections between the different actuators, it can be difficult to co-ordinate the inputs to achieve the desired result. As a consequence of these difficulties, MPD operations has been subjected to more and more automation and in particular model predictive control (MPC) in recent years.

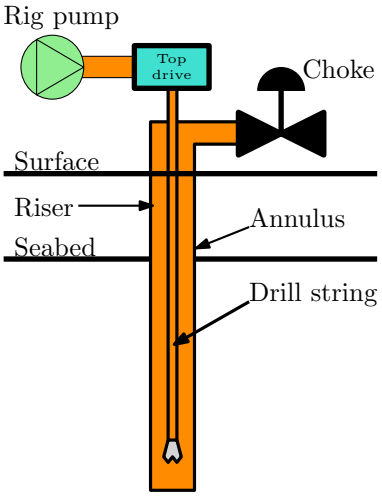

FIGURE 2.2: A simple MPD system with Rig pump and choke. Often equipped with a back pressure pump upstream the choke.

The simplest MPD system is a configuration similar to the system described in Section 2.1 with the exception that the riser is closed of by a choke, see figure 2.2. Here, a lighter mud is chosen to initially lower the BHP and then the choke opening is reduced to increase the pressure again. If any deviation in the BHP is detected in the setup the choke can be adjusted to compensate. This can be done manually or with a simple PI controller.

2.5 Dual gradient drilling

This thesis will deal with a variation of MPD called dual gradient drilling (DGD). DGD was developed in the 90's and is characterized by the use of two muds with

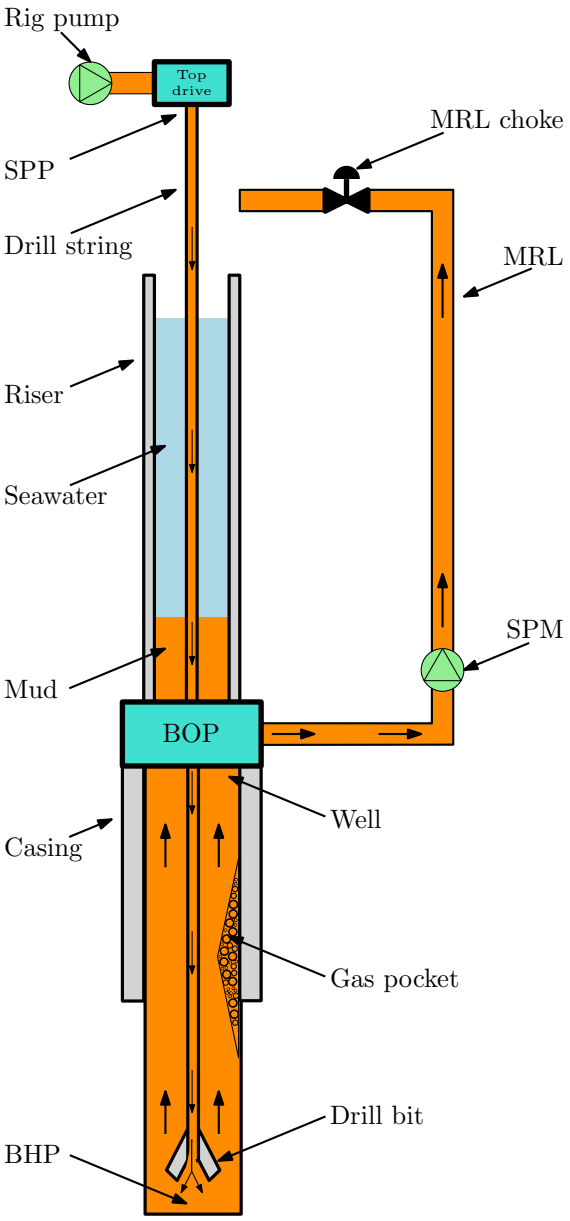

FIGURE 2.3: A schematical drawing of the dual gradient drilling system with gas pocket

different density. A lighter mud with density equal to seawater is used in the riser allowing use of a denser mud in the annulus in the well. This allows the pressure profile in the annulus to fit the ambient profile better which make it possible to drill longer sections. There are several configurations of DGD, but common for all of them is that the riser cannot be used as return line for the well-mud as this would cause the two muds to mix. Instead the mud is returned to the surface through a mud return line (MRL), see figure 2.3. Because the mud int MRL is

denser than the mud in the riser it is necessary to place a subsea pump module (SPM) at the bottom of the MRL in order to compensate for the difference in pressure. Without this pump the surface level between the two muds in the riser would be elevated too far up causing the BHP to rise above its set point. A similar issue may arise due to the in the drill string. If the rig pump is operating at a too low flow rate the dense mud will eventually displace the light mud in the entire riser. The reason way it never becomes a problem with normal flow rate is the increased friction losses.

Friction loss occurs in all pipes due to the no-slip condition [5]. Depending on weather the flow is laminar or turbulent the pressure loss/gain may be considerable. In a drilling system the flow is often turbulent in the drill string due to the small diameter and the high velocity. In the annulus, however, the flow is often laminar as the cross-section here is much larger causing a lower velocity. The friction loss is thus significantly higher in the drill string compared to the annulus, and the difference is sufficient to compensate for the denser mud if the flow is above a certain limit given by the systems current state.

2.5.1 Hydraulic model

To help understand understand the system dynamics it is important to have a derive a mathematical model which describes how the different flows and pressures are connected. A model describing a general DGD system can be found in [6]. However, in this thesis the focus will be on a DGD system where a gas kick has been detected. In these cases the system will be similar to the one in figure 2.4, where the annular room of the riser is closed off at the blowout preventer (BOP). Furthermore, the SPM is assumed to be directly connected between the remaining annulus and the MRL. These modifications makes it possible to use the hydraulic

equations derived in [7] with a minor modification to include the SPM:

$$\frac{V_d}{\beta_d}\dot{p}_{rig} = q_{rig} - q_{bit} \tag{2.2a}$$

$$\frac{V_a}{\beta_a}\dot{p}_{spm,us} = q_{bit} - q_{spm} \tag{2.2b}$$

$$\frac{V_r}{\beta_r}\dot{p}_c = q_{spm} - q_c \tag{2.2c}$$

$$M\dot{q}_{bit} = p_{rig} - p_{spm,us} - f_d(q_{bit}) - f_a(q_{bit}) + \rho_d g h_d - \rho_a g h_a \tag{2.2d}$$

$$p_{spm,ds} = p_c + f_r(q_{spm}) + \rho_r g h_r \tag{2.2e}$$

$$p_{dh} = p_{spm,ds} - \Delta p_{spm} + f_a(q_{bit}) + \rho_a g h_a \tag{2.2f}$$

where

- $V_\square$ is the drill string (d), annulus (a) or MRL (r) volume
- $\beta_\square$ is the drill string (d), annulus (a) or MRL (r) bulk-modulus
- $\rho_\square$ is the drill string (d), annulus (a) or MRL (r) average density
- $f_\square$ is the drill string (d), annulus (a) or MRL (r) frictional pressure drop
- $h_\square$ is the drill string (d), annulus (a) or MRL (r) height
- p_{rig} rig pump pressure
- p_{dh} downhole pressure (BHP)
- $p_{spm,us}$ pressure upstream SPM
- $p_{spm,ds}$ pressure downstream SPM
- $\Delta p_{spm} = p_{spm,ds} - p_{spm,us}$
- p_c choke pressure
- q_{rig} rig pump flow
- q_{bit} drill bit flow
- q_{spm} SPM flow
- q_c choke flow
- M is integrated density per cross section over the flow path

In this model equation (2.2a) to (2.2d) describes the dynamics and equation (2.2e) and (2.2f) describes the system at steady state. Three different control volumes has been used to derive these equations: the drill string, the annulus and the MRL. The first three equations stems from conservation of mass and the fourth from conservation of momentum.

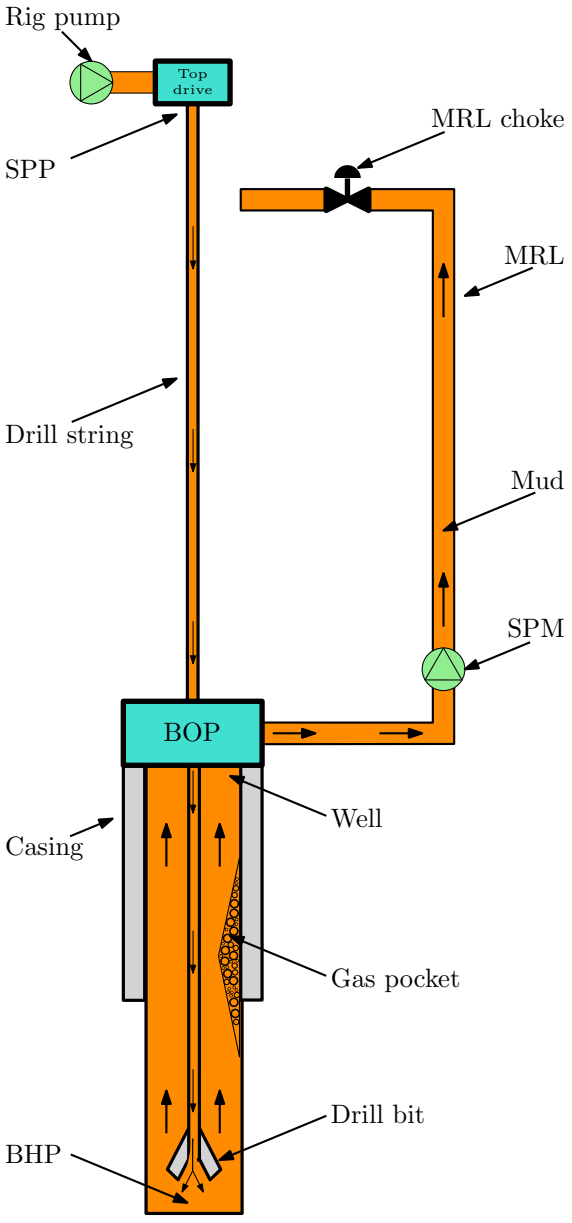

FIGURE 2.4: A schematical drawing of the dual gradient drilling system with the annular room in the riser closed off

The bulk-modulus β is the inverse of fluids compressibility and is related to the speed of sound c as stated in equation (2.3)[5]. The bulk-modulus will thus govern

the time constant of the system as indicated in the equations.

$$c = \sqrt{\frac{\beta}{\rho}} \tag{2.3}$$

From the steady state equations (2.2e) and (2.2f), it is possible to get a better understanding of how the system works. Whereas the flow comes from the rig pump, the pressure propagates from the choke. The BHP is determined form the choke opening, the speed of the SPM and the flow rate through the pipes, SPM and choke. The rig pump, however, is connected to the BHP indirectly through manipulating those flow rates in the annulus and MRL. This fact makes it difficult make a simple model from the rig pump flow rate to the BHP.

2.6 Instrumentation

In order to control the BHP it is necessary to have either a direct measurement or a an estimation of the pressure. Due to cost issues it is common to use an estimator which uses hydraulic models and measurements above the well to determine the BHP. One variant of a BHP estimator can be found in [7] where an adaptive observer is developed. However, since implementation of an BHP estimator is outside the scope of this thesis, it is assumed that the BHP be is measured directly with, for instance, a wired drill string.

2.6.1 Gas kick measurement

When a drilling system is subjected to a gas kick it is important to detect the influx in order to take the appropriate measures to stop the influx and ventilate the gas out safely. The issue of detecting a kick can be difficult to solve and in this thesis it is assumed to be known in all simulations. An adaptive observer for kick detection can however be found in [8].

In all the simulations the gas fraction in the SPM is assumed to be known in order to switch it off in the periods where it is impeded by the gas. The gas fraction is, however, difficult to measure in a real system because it require the use of a multiphase meter. Not only is the multiphase meter very expensive, it is also rather inaccurate with as much as 10% relative error[9]. According to Wikipedia[1] the cost of a multiphase meter lies between US$100,000 and US$500,000 whereas the feasible price for the drilling companies lies somewhere around US$50,000. The measurement is nevertheless included as the author hasn't come up with any alternative.

[1] `http://en.wikipedia.org/wiki/Multiphase_flow_meter`

Chapter 3

Model predictive control

Model predictive control is in the category of advanced controllers which mostly is used in large process industries. The reason for its success is the ability to operate large multivariable systems closer to the limiting constraints. This is possible because the MPC has mathematical models of the system which which makes it able to calculate where the system states and inputs must be to optimize production and at the same time abide the system's constraints.

The MPC comes in many variations, some more computational expensive than others. The demanding MPCs are those with nonlinear models, large state vectors and long prediction horizons. Nonlinear models requires the MPC to use demanding algorithms which increases the the computation time considerably. Furthermore, the size of the state vectors and prediction horizon determines the size of the matrices which adds to the computational time as well. These drawbacks, in addition to the big costs of developing and implementing the MPC, are main disadvantages.

As in all variations of the MPC the underlying mathematical structure is a optimization problem with a objective function which is subjected to certain constraints. The objective function, also refereed to as the cost function, is an expression which comprise all the controlled variables (CV) and manipulated variables

(MV) and their corresponding set points and weights.[1] In order to minimize wear on the actuators the derivative of the MVs are added to the objective function so that the MVs are moved as little as possible. All the variables are usually squared in the objective function as seen in equation (3.1a). This is mostly due to convention, but also the fact that it aids to lower the error variance.

By choosing weight matrices Q_y, Q_u and P as diagonal matrices with only positive elements the matrices will always be positive semi-definite. Not only does this make the objective function convex, but it also makes weighting the individual CVs and MVs easy.

3.1 Linear MPC

A linear MPC uses a linear model to calculate how the MVs should be changed in order to bring the system to optimal state. The linear models are mathematical descriptions of the system which stipulates how a change to the MVs will affect to CV. The models may be implemented in many ways, for instance as step responses models or state space models. Because the system model, which is found in equation (3.1e), is linear, the objective function is convex and the inequality constraints are concave, the optimization problem is in the category of convex quadratic programming. The fact that the optimization problem is convex allows the use of simple iterative optimization algorithms such as active set methods or interior point methods[10].

[1] If one of the variables don't have either a set point or weight it is omitted from the objective function.

$$\underset{\Delta u}{\text{minimize}} \quad y_{dev}^{\top} Q_y y_{dev} + u_{dev}^{\top} Q_u u_{dev} + \Delta u^{\top} P \Delta u \tag{3.1a}$$

$$\text{subject to} \quad u_{min} < u < u_{max} \tag{3.1b}$$

$$\Delta u_{min} < \Delta u < \Delta u_{max} \tag{3.1c}$$

$$y_{min} < y < y_{max} \tag{3.1d}$$

$$y = M(y, u, d, v) \tag{3.1e}$$

The optimization problem in equations (3.1) is the formulation that is implemented in SEPTIC [11] which is the MPC-tool used in this thesis. The subscript, dev, indicates that it is the deviation from the variables set point that is used. Note that this formulation doesn't specify an explicit prediction horizon. When augmenting the objective function (3.1a) with the prediction horizon it will take the form of equation (3.2).

$$\sum_{t=0}^{N-1} y_{dev,t+1}^{\top} Q_y y_{dev,t+1} + u_{dev,t}^{\top} Q_u u_{dev,t} + \Delta u_t^{\top} P \Delta u_t \tag{3.2}$$

In this formulation it is assumed that the current CVs, y, are either measured or estimated, and it is the current input which is computed, hence the plus one increment on the CVs.

The constraints (3.1b) and (3.1c) are usually implemented as "hard" constraints, that is, they will never be relaxed in order to minimize the deviations in the CVs. Furthermore, these constraints usually stems from physical limitations in the actuators which makes a violation of them impossible in practice. In contrast, the constraints on the CVs found in equation (3.1d), are in most implementations of the MPC possible to violate. This is common practice because the mathematical solver will terminate the operation if the problem becomes infeasible which then will leave the system uncontrolled. So in order to make the controller obey these constraints as good as possible the constraint is added to the objective function with a relatively high weight to minimize the amount of violation.

A procedure of a typical mpc algorithm[12] can be found in Algorithm 1. This does not describe any of the advanced solving procedures found in most implementations in the industry, but it describes the main strategy used be the solver. Note that the prediction horizon moves forward as time progresses.

Algorithm 1 Linear MPC with state feedback

for t=0,1,2,... **do**
  Get the current y_t.
  Solve the convex QP problem on the prediction horizon
    from t to $t + N$ with y_t as initial condition.
  Apply the first control move u_t from the solution above.
end for

3.2 Priority hierarchy

Most MPC tools found in the industry has some sort of priority hierarchy to determine which constraints to violate if it becomes impossible to honour all of them. As mentioned in the previous section some of the constraints are hard, i.e. impossible to violate. These constraints will therefore get maximum priority. The typical constraints to violate are those which limits the CVs as these generally can be violated. The exception is CVs like humidity which can't exceed 100% or the water level in a vessel which can't rise above the ceiling.

In list below the priority list implemented in SEPTIC is shown. Entries 1 and 2 will never be violated, nor will entry number 3 provided that it is implemented true to the physical constraints. A disturbance could otherwise violate point 3. The constraints and set points[2] in entry number 4 may be violated if no other feasible solution exists. This would typically be caused by disturbances. If there are two or more constraints that may be violated, SEPTIC will violate the one with the lowest priority, i.e. the constraint or set point with the highest number.

1. MV rate of change limits

[2]In SEPTIC the term "ideal value" is used instead of set point when dealing with an MV.

2. MV high and low limits
3. CV hard constraints
4. CV and MV set point, and CV high and low limit with priority from 1 to 99

3.2.1 SEPTICS' handling of priorities

When SEPTIC is calculating its next control move it will start by computing where the variables needs to be in steady state to minimize the objective function. If all constraints and set points can be met SEPTIC will disregard the priorities and start computing the the least expensive way to get from the current state to the calculated steady state. This will in practice mean that SEPTIC will minimize the derivative part of the objective function (3.2) in the prediction horizon.

If on the other hand SEPTIC finds that it is impossible to abide all constraints, the priority hierarchy comes into play. By looking at the models SEPTIC can determine which constraints that will oppose each other in steady state. Of these constraints the one with lowest priority will be removed from the optimization problem and then a new steady state calculation will be computed. If the optimization problem still is infeasible the second lowest priority constraint is removed and so on. Afterwards, SEPTIC will minimize the modified objective function to find the optimal path to steady state. At the next time instant the optimization problem will return to its original version and the procedure will be repeated if necessary.

3.3 Step response models

The process of developing accurate models that describes the system to be controlled can be very time consuming and thus costly. Especially in large systems with many variables the expense might be to big even when taking the improved performance into account.

In the industry a very simple solution has become very popular. Instead of deriving analytical models using different kind of conservation laws the model is simply created by a step response. When the system operates at steady state one of the inputs is subjected to a step which then will propagate through the system. The resulting movement at the output is called the step response and it describes how the input influences the output. A step response model from every input to every output is needed to get a full description of the system. When the controller predicts ahead it will scale the models in accordance with the change of inputs. The principle of superposition is employed whenever two or more inputs are being used to control one of the outputs.

Note that this procedure require a open loop stable system as the system needs to converge to steady state before and after the step.

3.3.1 Dynamic models

Although this thesis utilizes a linear MPC to control the hydraulic system, the actual system is far from linear. As will be shown later, near every actuator and disturbance acts nonlinearly on the BHP. Due to robustness caused by the feedback a linear MPC will, nevertheless, perform good in many cases. However, the challenges encountered in this problem has shown that the model error is too big in order to obtain satisfying performance.

To accommodate these challenges dynamic models was implemented. For instance, the pressure over a choke will be much more sensitive reducing its opening from 100% to 90%, than reducing it from 40% to 30%. By making the model dependent on the choke opening it is possible to scale the gain in order to better fit the model to the actual choke characteristics. This strategy is called gain scheduling and it can significantly improve the control performance.

It is also possible to correct the time constant of the model. If, for instance, the bulk-modulus of a fluid changes due to influx to the well, the time constant could be corrected provided that the change is observable.

When implementing such models in a linear MPC a linearisation will be made at every time instant. That is, the controller will have updated models at all times, but when predicting ahead the algorithm will not take into account that the model may change in the future. Due to this weakness the first part of the prediction may be fairly good, however, the last parts might well be far from ideal.

3.4 MV blocking

MV blocking is widely used in industrial MPC implementations. By dividing the prediction horizon into sections, or blocks, of several time instants the number of decision variables in the optimization problem is reduced accordingly. The resulting prediction of control inputs will then be constant in each section which obviously will lead to reduced accuracy. The upside, however, is that provided that the blocking intervals are chosen sensible, the decrease of accuracy becomes negligible, and the computation time at each time instant will get significantly reduced.

The blocking may be chosen differently for each MV as a fast response may require more frequent changes at the beginning of the horizon than slow responses. To further adapt to these requirements it is possible, and quite common, to use varying size of the intervals, see figure 3.1. As the responses usually are fast changing in the beginning it is desirable have smaller intervals here than further out on the horizon.[13] Another argument for this practice is that the accuracy at the end of the horizon usually is lower anyway due to model errors.

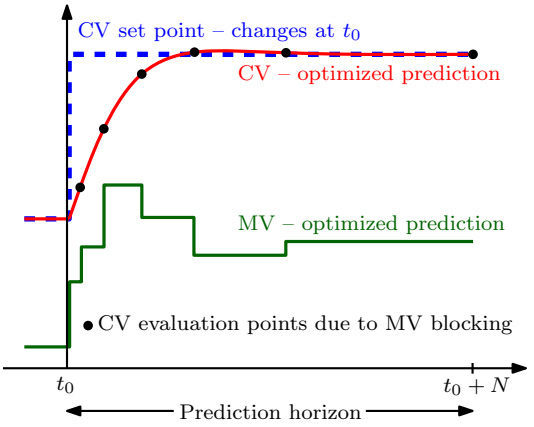

FIGURE 3.1: Blocking in septic. The figure is taken from [11].

3.4.1 Prediction horizon

The length of the prediction horizon is an important tuning parameter in an MPC. As with blocking a compromise between accuracy and fast computation time must be made such that the important dynamics are covered in the prediction, and the computation time stays far below the sampling time. With first order responses it is common to choose a prediction horizon equal to 3 times the time constant of the response, plus any time delay. With modern computers such prediction horizons rarely pose any problems regarding computation time. In addition, since long prediction horizons are used on systems with corresponding long time constants, it is reasonable to assume that the sampling time in this cases is longer than for fast systems. If the system comprise both fast and slow responses a solution could be to customize the length of the horizon to each MV.

Chapter 4

The Model

The model used in this thesis is a model of the controlled mud pressure test at Statoil's Troll platform. The model has been thoroughly developed in Dymola by Statoil and features realistic multiphase flow characteristics. Some modifications to the model has been made by the engineers at Statoil in order to obtain the desired configuration.

4.1 System configuration

The drilling system used in this thesis is a modified version of a DGD system which purpose is to describe how a drilling well behaves when a gas kick is detected and propagating up the annulus. The procedure used to handle a gas kick will in this thesis, will alter the normal configuration as mentioned in Section 2.5.1. When a kick is detected the the annular room in the riser is closed off from the well at the BOP resulting in the system that can be found in 2.4.

When the system turns into this state the system does not have two gradients any more and the BHP is now determined by the hydro pressure in the annulus and the MRL, in addition to the choke pressure and the SPM pressure difference.

4.2 The Dymola model

An illustration of the system modelled in Dymola can be seen in Figure 4.1.

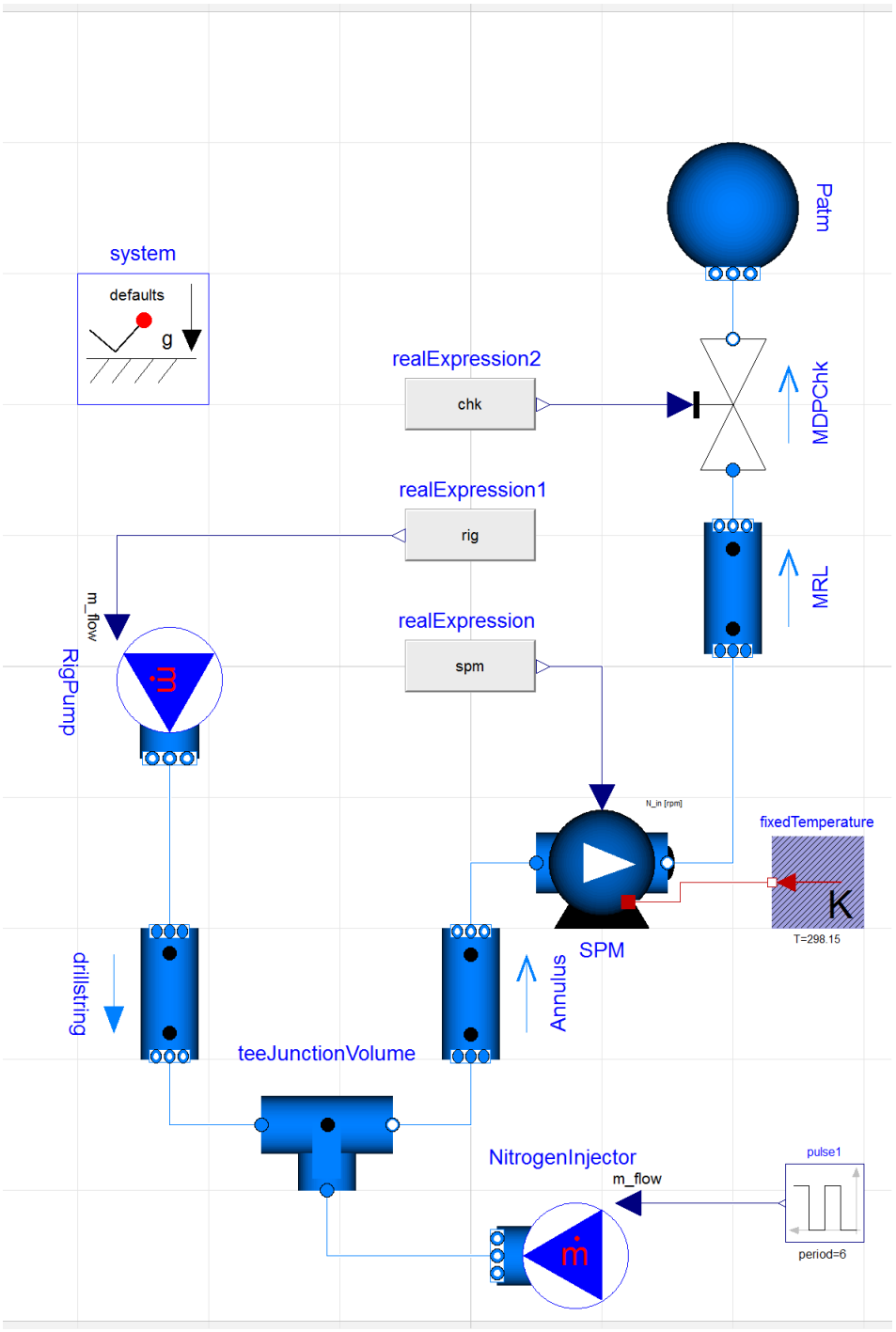

FIGURE 4.1: The drilling system modelled in Modelica with Dymola.

Starting upstream the rig pump is modelled as an ideal mass flow pump which means that no matter how the conditions at the connected drill string are, the pump will push out a mass flow determined by the pump's input. The drill string leads the mud down 1280 meters to a junction point where the drill bit would be in a real system. The drill string is modelled as a pipe without any sort of joints that would affect the flow in practice. The junction point at the bottom allows gas to enter the system in the same manner the mud entered at the top. Unlike the other pipes the junction point does not feature any advanced flow characteristics like friction or roughness. Its volume measure 100 litres.

Attached the drain of the junction point is the annulus. As its name implies this pipe should be annular, however, it is modelled as a regular pipe with its parameters adjusted to fit the reality. Next in line is the SPM which is attached directly to the annulus as the BOP is omitted. The SPM used in this model is a centrifugal pump. Finally, the mud is led through the MRL to a choke valve before exiting into a mud pit with atmospheric pressure.

4.2.1 The pipe model

All the pips, i.e. the drill string, annulus and MRL, utilizes the same computer model, although with different parameters. The drill string has, unlike the other pipes, a one way valve which only effect is to prevent reverse flow.

Table 4.1: Specifications of the pipes used in the model

	Length	Diameter	Elements	Roughness	Friction adjustment factor
Drill string	1280 m	12.09 cm	5	5 mm	4.5
Annulus	920 m	29.36 cm	60	6 mm	3
MRL	360 m	15.24 cm	20	< 0.1 mm	3

In addition to the specifications in Table 4.1 all the pipes has a slip factor of 0.7, that is, the gas will move about 43% faster than the mud. The number of elements determines the resolution of the flow. With more elements it is possible to capture more variations in flow and pressure along the pipe. This is particularly important

because it allows the gas kicks to get a more realistic distribution in the annulus and MRL, hence the increased number of elements in these pipes. A trade-off has, however, been made here as more elements increases the number of states and equations in the model and thus increases the computation time.

The roughness, denoted ϵ, is a parameter that describes the average height of asperities in the pipe walls. Wear will in most cases increase this number during the pipe's operation time. The roughness parameter is important in turbulent flows as it is included in Colebrook's equation (4.1) which computes the Darcy friction factor[1][5, 14].

$$\frac{1}{\sqrt{f}} = -2\log_{10}\left(\frac{2.51}{\mathrm{Re}\sqrt{f}} + \frac{\epsilon}{3.7}\right) \tag{4.1}$$

where Re is the Reynolds number. This friction factor must not be confused with the friction adjustment factor from the table which will be explained shortly. The Darcy friction factor is used to find the relation between the fluid velocity, V, and the head loss due to friction, h_f, as seen in (4.2).

$$h_f = f\frac{L}{d}\frac{V^2}{2g} \tag{4.2}$$

where L is length of the pipe and d is the diameter.

The friction adjustment factor is dimensionless parameter used in this pipe model to adjust the flow due to the friction in the pipe. In the model the parameter adjusts the flow as shown in equation (4.3).

$$\dot{m} = \frac{1}{\sqrt{f_{af}}}\mathrm{Re}\cdot\pi\frac{d}{4}\mu \tag{4.3}$$

where $\dot{m}$ is the mass flow rate, f_{af} is the friction adjustment factor, and μ is the viscosity.

[1]Note that some implementations use the Fanning friction factor which is one-fourth of the Darcy friction factor.

4.3 The subsea pump module

To compensate for the higher hydrostatic pressure in the MRL relative to the annulus in the riser a subsea pump module (SPM) is placed at the bottom of the MRL down at the seabed. This module comprise three centrifugal pumps in series which together delivers a pressure drop of approximately 20 bar at normal operation. For simplicity the SPM is modelled as one pump in the Dymola model with revolutions per minute (rpm) of the impeller as MV. In a real pump it will take the impeller some time to adjust to the new angular velocity, nevertheless, in the model this velocity can be set instantly although this is never done due to constraints implemented in SEPTIC.

In a centrifugal pump the flow is dependent on not only the impeller velocity, but also on the pump's head which isn't the case for positive displacement pumps. In this context the head is related to the hydrostatic pressure and can be obtained by dividing the pressure difference with the fluid's density and the acceleration of gravitation. To derive a mathematical model of the pump it is common to use the similarity rules to approximate a function for the head to experimental data[5]. The model used in this thesis has a function on the form seen in equation (4.4).

$$f_{spm}(q_{spm}, \omega_{spm}) = c_0\omega_{spm}^2 - c_1\omega_{spm}q_{spm} - c_2q_{spm}^2 \tag{4.4}$$

Where f_{spm} is the head, q_{spm} is the volume flow rate and ω_{spm} is the angular velocity of the impeller. The parameters c_0, c_1 and c_2 is determined by Dymola by defining three operation points. Table 4.2 shows these operating points with a nominal rotational speed of 1500 rpm.

Table 4.2: Three operations points defining the pump characteristics.

Rotational speed 1500 rpm			
Flow	1000 l/min	2500 l/min	5000 l/min
Head	276 m	268.5 m	255 m

With these data the parameters becomes: $c_0 = 1.25 \cdot 10^{-4} m \cdot \text{min}^2$, $c_1 = 3.10 \cdot 10^{-6} m \cdot \text{min}^2/l$ and $c_2 = 1.00 \cdot 10^{-7} m \cdot \text{min}^2/l^2$. The knowledge of these pump

characteristics will be of great value when creating prediction models in SEPTIC later. Pump curves for some selected rotational speeds can be found in Figure 4.2.

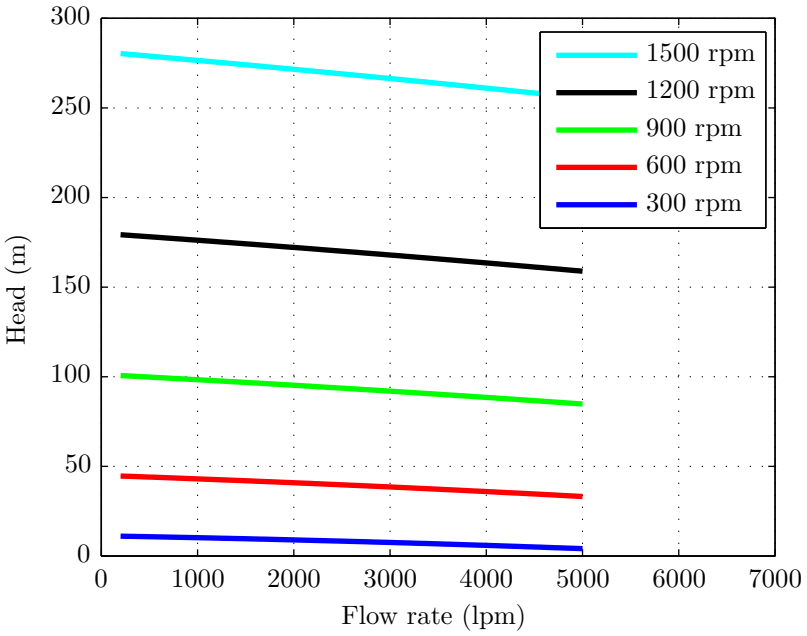

FIGURE 4.2: Pump curves for some selected rotational speeds. Note that the curves are almost linear in the operational region.

When the gas proportion of the fluid begins to rise to a substantial level a centrifugal pump will start to loose its head even though ω_{spm} and q_{spm} are constant. To incorporate this effect into the SPM model, equation (4.4) is augmented with a gas efficiency factor $\eta(\alpha_{pG})$ where α_{pG} is the gas fraction, see equation (4.5).

$$f_{spm}^{gas}(q_{spm}, \omega_{spm}, \alpha_{pG}) = \eta(\alpha_{pG}) f_{spm}(q_{spm}, \omega_{spm}) \tag{4.5}$$

In the model used here it is assumed that the gas efficiency factor takes the form:

$$\eta(\alpha_{pG}) = \begin{cases} 1 & \alpha_{pG} \leq 0.1 \\ -10\alpha_{pG} + 2 & 0.1 < \alpha_{pG} < 0.2 \\ 0 & \alpha_{pG} \geq 0.2 \end{cases} \tag{4.6}$$

where the the head is unaffected with a gas fraction of less than 10% and decreases linearly to zero as the gas fraction increases to 20%, see Figure 4.3.

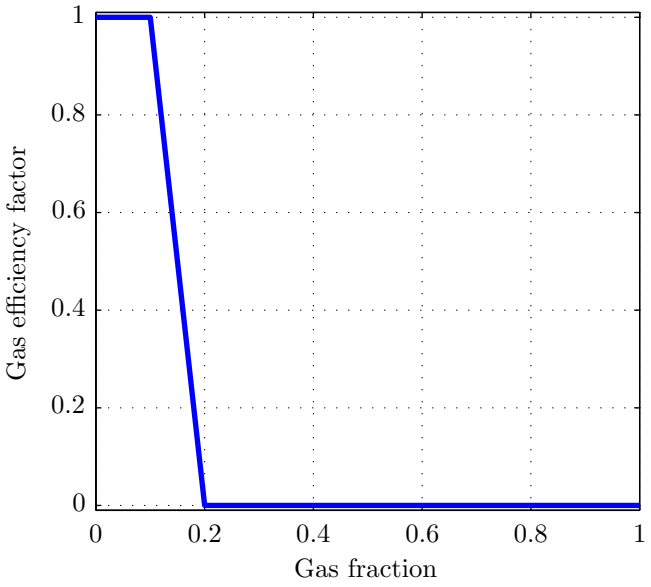

FIGURE 4.3: Plot of the gas efficiency factor which makes the SPM loose head when subjected to gas

4.4 The choke valve

When choosing the choke valve it is important to select appropriate characteristics and size. The choke characteristics depends on which mechanism used and describes the relation between the flow and the choke opening with the pressure drop held constant. In this thesis a piecewise linear choke has been used at the end of the MRL, see Figure 4.4. This curve indicates that there are alomst no nonlinearities above choke openings of 25%. Because the flow becomes almost zero below 25% opening the operational begins at this point unless the choke needs to closed.

The size of the choke is important to get the desired performance. Choosing a choke too big could hurt the system in two ways. First, a oversized choke would have to operate near to its closed state causing the choke gain to be unnecessary high. In many cases this could lead to instabilities or at least damaging oscillations.

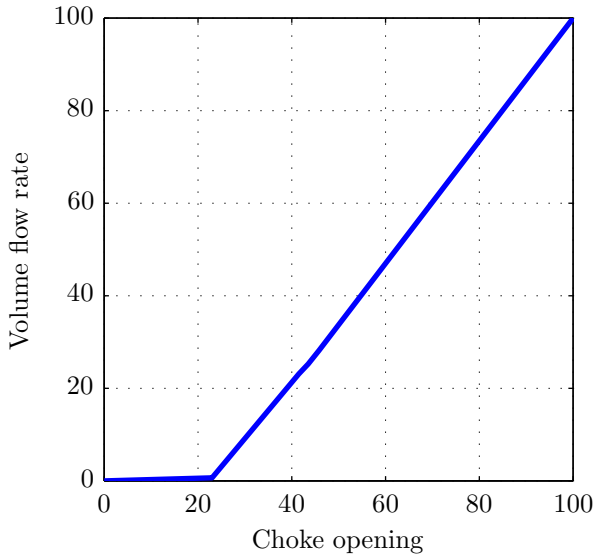

FIGURE 4.4: The figure shows how the volume flow is affected by the choke opening when the the pressure drop is constant. This function is implemented in the Dymola model.

The second way a oversized choke could affect the system is the fact that the choke would operate at small openings where seal friction can be larger. This friction causes a dead band which can be exaggerated into violent oscillations due to the high gain[15].

If the choke is chosen too small it will put debilitating constraints on the system as the choke wont be able to drain enough fluid at the desired pressure drop.

In the Dymola model the US flow coefficient, C_v, is used to specify the choke size. The formulation[5] in which this coefficient is used is given in equation (4.7).

$$C_v = Q\sqrt{\frac{SG}{\Delta p}} \tag{4.7}$$

Here is SG the specific gravity, that is, the ratio between the density of the fluid at hand and water. Moreover is Q the volume flow rate and Δp the pressure drop. In the model used in this thesis C_v is set to 100, where one C_v is one US gallon per minute of 60° F water with a one psi pressure drop.

4.5 The medium

The fluids used in the model are a water based drilling mud and nitrogen which serves as the gas in the kicks. The mud is a expensive liquid which needs several properties in order to create the desired flow type, lift up cuttings the annulus and create the the desired hydrostatic pressure. The nitrogen is modelled as a ideal gas and the mud specifications can be found in Table 4.3.

Table 4.3: Specifications of the water based mud

Density at 1.01 bar	1250 kg/m^3
Speed of sound	1000 m/s
Viscosity at 20°C and 50°C	0.01 Pa $\cdot$ s and 0.0055 Pa $\cdot$ s
Heat capacity	4181.3 J/(kg $\cdot$ K)

4.6 Emulation of a gas kick

A gas kick is normally occurring when the BHP drops below the pore pressure. However, since the scope of this thesis only concern the issues arising as the gas propagates up the return lines, and not the kick itself, a simple method for administrating the kicks has been made.

The following procedure is started at the beginning of every simulation investigating a kick.

1. At t=0s: Set Rig pump to 1000 lpm, SPM to 1150 rpm and choke to 100 %.
2. At t=590s: Set Rig pump to 0 lpm.
3. At t=600s: Set gas injector to the desired gas influx.
4. At t=606s: Set gas injector to back to 0.
5. At t=620s: Set Rig pump to 1000 lpm.

This method creates violent pressure transients up to about 2 minutes after the last rig pump action. At this point the control problem begins.

The Dymola model only allows the user to specify how much mass of gas that will be pumped into the system. As the convention in the industry is to measure influx in oil barrels (159 litre), the kick size is converted to this unit by assuming a BHP of 142 bar. This means that when it later in the thesis is referred to a 1 barrel kick, it is equivalent to 25kg of gas.

Chapter 5

Controller design

In the predecessor of this thesis a reference case where the drilling system was controlled by a PI controller was made. This case is included here as well in order to assess the performance of the MPC. The configuration of the reference case is elaborated in Section 5.1.

5.1 PI controlled reference case

In this simple control case there is only one MV, the choke, and one CV, the stand pipe pressure (SPP). Of the remaining actuators the SPM is maintaining constant speed at 1150 rpm and the rig pump keeps a constant flow rate of 1000 litre per minute (lpm).

The SSP can be used as an estimator of the BHP in this case due to the constant flow rate, see equation (5.1).

$$p_{dh} = p_{rig} + \rho_d g h_d - f_d(q_{bit}) \tag{5.1}$$

where p_{rig} is the pressure at the rig pump referred to as SPP.

Because q_{bit} is constant there will always be a fixed pressure drop from the BHP to the SPP. And since the hydrostatic pressure and the frictional pressure accounts for approximately 114 bar, the BHP set point of 142 bar corresponds to a SPP set point of 28 bar.

5.1.1 Tuning of the PI controller

The PI controller used in the reference case featured anti wind-up because the choke was saturated at several points during simulation. The controller was tuned by making qualified guesses of the gain and integration time and then adjusted until decent performance was achieved. In this case decent performance means that saturation and rate limits became the limiting elements preventing the controller to perform any better.

The tuning parameters was $K = 10$ and $T_i = 60$, where K is the controller gain and T_i is the integral time.

5.2 Configuration of the MPC

As mentioned earlier the MPC will be controlling one CV, the BHP, with three MVs, the rig pump, SPM and choke. Instead of having additional CVs to keep control of the pressure profile, like it was done in the preceding project, the rig pump and choke has ideal values which the controller will try to maintain. In addition the SPP is included as a CV with only a low threshold to prevent the mud level from falling in the drill string. See Section 2.5 for more information. Only the rig pump will be controlling this CV.

5.2.1 Variable limit in SPM – Multiphase meter

When the SPM is impeded by gas it is important to force the controller to spin down the pump rather than up, which it might do to compensate for the pressure

loss. In order to accomplish this it is assumed that a multiphase meter is measuring the gas fraction in the SPM so the controller knows when to spin it down and up again. Equation (5.2) shows how the high threshold of the SPM is implemented in SEPTIC.

$$\text{limit}_{\text{spm}} = \begin{cases} 2000 & \alpha_{pG} \leq 0.1 \\ -17000\alpha_{pG} + 3700 & 0.1 < \alpha_{pG} < 0.2 \\ 300 & \alpha_{pG} \geq 0.2 \end{cases} \tag{5.2}$$

where α_{pG} is the gas fraction.

5.3 Step response models

A model predictive controller relies on models from the MV's to the CV to calculate the control moves. The models used here are time varying step response models which has been developed through numerous experiments. Not only does the models has varying gain, the time constants are varying as well.

5.3.1 The rig pump gain

The rig pump is connected to the BHP indirectly through altering the flow in the pipes and equipment in the return lines. As explained earlier the volume flow rate will affect friction loss in the pipes, the operating point in the pump curves in the SPM, as well as pressure drop in choke. It is obviously possible to derive an expression for the resulting pressure change given the change in rig pump flow, however, such a model will be unnecessary complicated as it will be dependent on the states of the other MVs. In addition, the gas kicks will undoubtedly complicate the model even further, consequently making a linear MPC less applicable.

Instead, an experimental model has been made. By varying the rig pump flow with increments of 100 lpm in the interval from 700 to 1400 lpm and logging the

resulting BHP, the data has been used to develop a mathematical function which describes the correlation. During these experiments all the other MVs was fixed at their ideal values. Figure 5.1 shows the measured points and a fitted curve which is used in model updates.

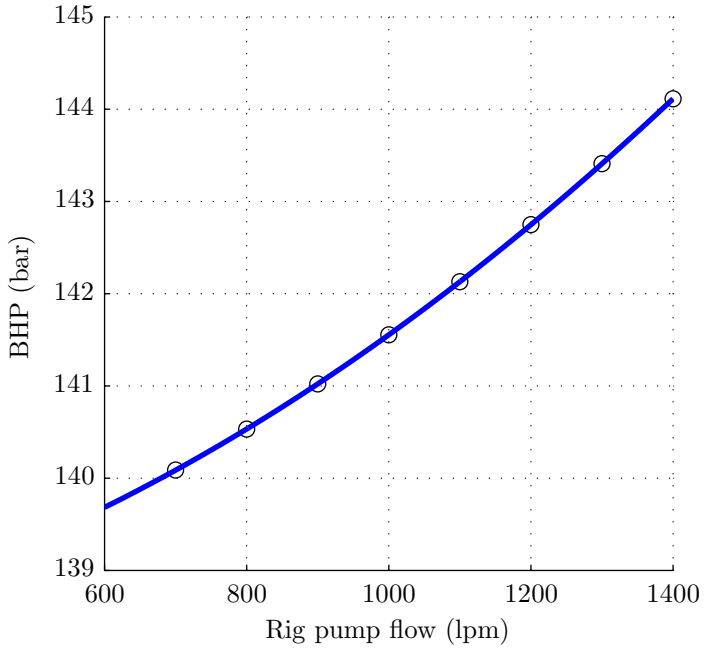

FIGURE 5.1: Empirically obtained correlation between rig pump flow and the BHP.

The curve fitting resulted in the following second order polynomial (5.3).

$$f_{BHP}(q_{rig}) = 2.15 \cdot 10^{-6} q_{rig}^2 + 1.23 \cdot 10^{-3} q_{rig} + 138 \tag{5.3}$$

By differentiating f_{BHP} with respect to q_{rig} we can obtain the expression the gain from the rig pump to BHP, see equation (5.4).

$$G_{rig}^{BHP} = \frac{\mathrm{d}f_{BHP}}{\mathrm{d}q_{rig}} = 4.30 \cdot 10^{-6} q_{rig} + 1.23 \cdot 10^{-3} \tag{5.4}$$

where G_{rig}^{BHP} is the gain from the rig pump to the BHP.

This function was implemented in SEPTIC to specify the gain. A plot of the function can be found in Figure 5.2.

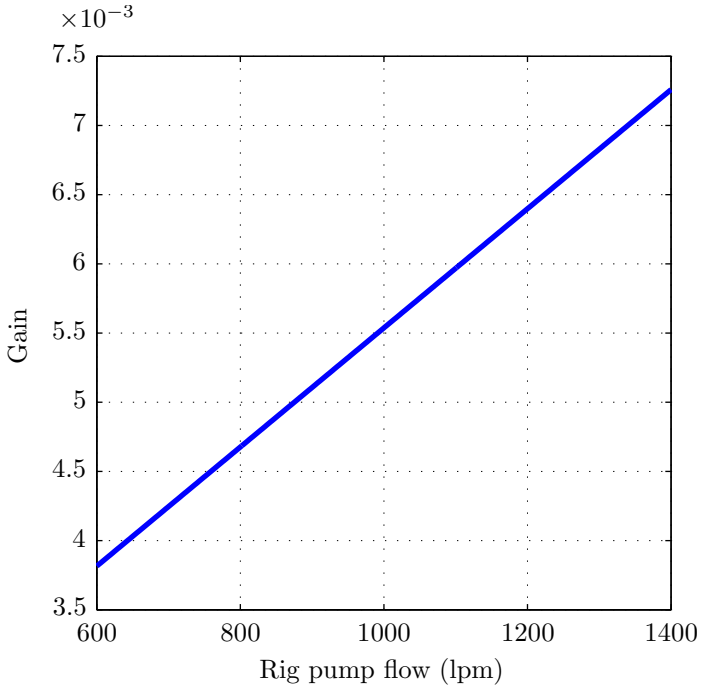

FIGURE 5.2: The figure shows how the gain from the rig pump the BHP changes as the flow changes.

5.3.2 The subsea pump module gain

The gain of the rig pump can be derived from the pump curves specified in Section 4.3. By assuming that the hydrostatic pressure, i.e. ρgh, in the annulus and MRL are fixed, it is clear that the head of the SPM will be proportionate the BHP. The SPM is modelled with head loss when subjected to fluid containing gas which will make the model misleading. However, because the SPM mostly will be in idle state in these periods, it is not necessary to include effect of the gas in the MPC model.

By looking at equation (4.4) restated below, it is clear that the model must be made with a specific predetermined flow as the the flow through the SPM q_{spm} is assumed unavailable.

$$f_{spm}(q_{spm}, \omega_{spm}) = c_0\omega_{spm}^2 - c_1\omega_{spm}q_{spm} - c_2q_{spm}^2$$

By taking the derivative in the same manner done with the rig pump the Gain from the SPM to the BHP is given by equation (5.5).

$$G_{spm}^{BHP} = -\rho g \frac{\mathrm{d}f_{spm}}{\mathrm{d}\omega_{spm}} = -9.81 \cdot 1250(2 \cdot 1.25 \cdot 10^{-4}\omega_{spm} - 3.10 \cdot 10^{-6}q_{spm})/10^5 \quad (5.5)$$

When setting q_{spm} equal to 1000 lpm, which is the average flow in the SPM's operational time, the gain has become a linear curve and can be observed in Figure 5.3.

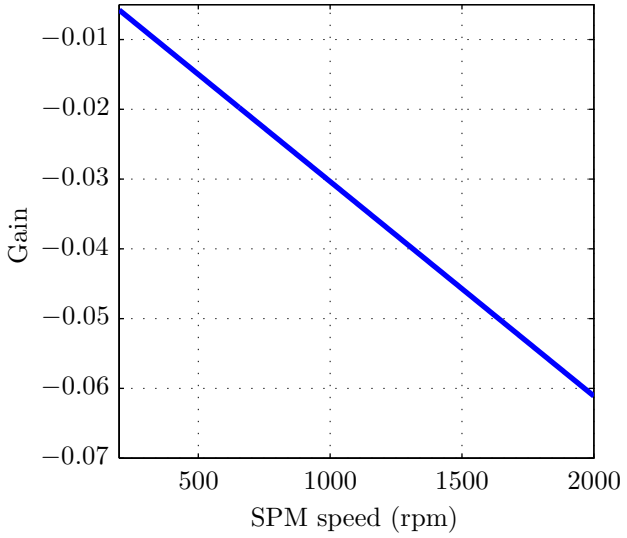

FIGURE 5.3: The figure shows how the gain from the SPM the BHP changes as the rotational speed changes.

5.3.3 The choke valve gain

The most important model is the one describing the relation between the choke and the BHP. As will be shown shortly, the gain is changing considerably across the choke range.

A choke model can be developed by applying Bernoulli's principle on a choked flow. Here we assume that the choke characteristics is on the form[5]:

$$Q = C_d A_{opening} \sqrt{\frac{\Delta p}{\rho}} \tag{5.6}$$

where C_d is the discharge coefficient and $A_{opening}$ the area of the choke opening. By collecting C_d and $A_{opening}$ into one function dependent on the choke opening z_c as defined in Dymola, the resulting choke equation becomes:

$$Q = g_c(z_c) \sqrt{\frac{\Delta p}{\rho}} \tag{5.7}$$

$g_c(z_c)$ is then estimated from experiment where the rig pump is changing flow two times and the choke is stepped up and down between 35 and 100 %. The result can be found in Figure 5.4.

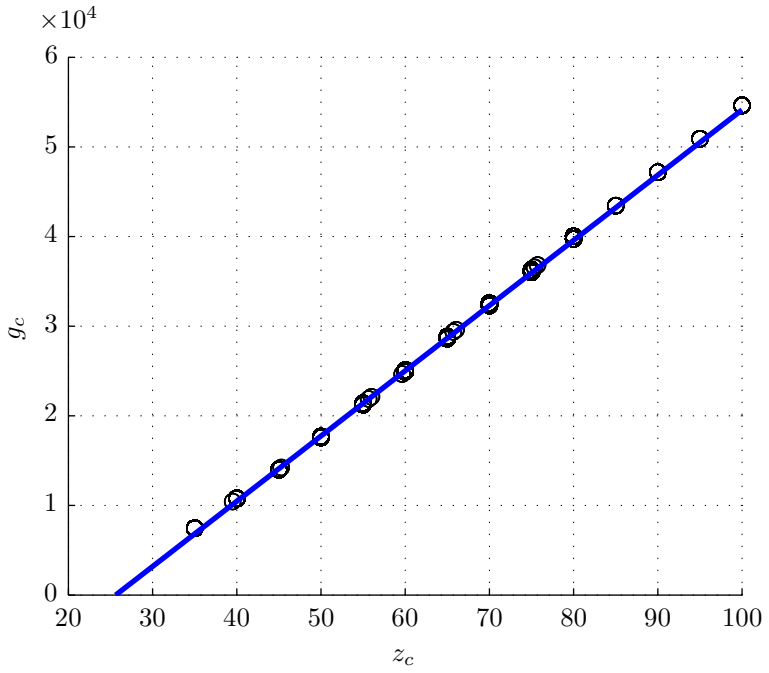

FIGURE 5.4: The figure shows the curve fitting of g_c as a function the choke opening z_c in %.

The blue graph, g_c, is given in equation (5.8).

$$g_c(z_c) = 727.82 z_c - 18645.3 \tag{5.8}$$

Equation (5.7) is then solved with respect to Δp and differentiated with respect to z_c to obtain the gain, see equation (5.9)

$$G_{chk}^{BHP} = \frac{\mathrm{d}}{\mathrm{d}z_c}\left(\frac{\rho Q^2}{g_c^2(z_c)}\right) = \frac{-1250 \cdot 727.82 \cdot 1000^2}{(727.82 z_c - 18645.3)^3} \tag{5.9}$$

A plot of the gain can be found in Figure 5.5

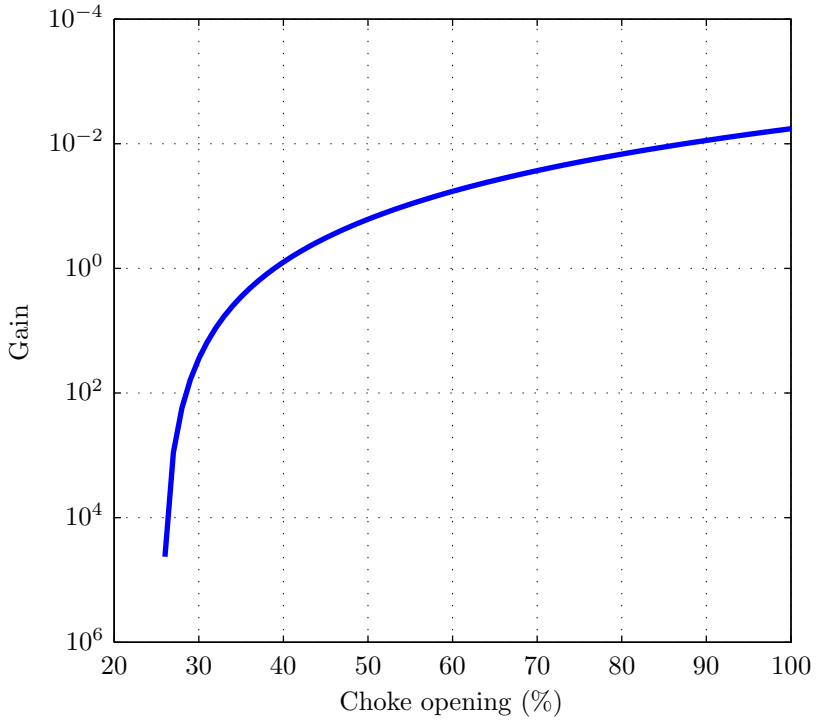

FIGURE 5.5: The curve shows the gain from the choke to the BHP in a logarithmic plot.

5.3.4 Adjusting the models for gas kicks

Although the gain scheduling implemented so far has improved the performance significantly, there were still issues regarding oscillations and large deviations as the gas was about to exit the system. An attempt to accommodate these problems was done by integrating the difference between mud mass flow out of the system and flow into the system, and investigate whether it was a correlation between the

integral and time constants and gain, see equation. The idea is that the integral will be almost proportional to the gas kick volume.

$$V_{kick} \propto \int_{Start}^{End} \dot{m}_{chk} - \dot{m}_{rig} \tag{5.10}$$

where V_{kick} is the volume of the gas, $\dot{m}_{chk}$ is the mass flow through the choke and $\dot{m}_{rig}$ is the mass flow from the rig pump. The integral starts and ends with the simulation.

Numerous simulations was conducted with varying sizes of kicks to estimate the correlation between the kick volume and the models. Kicks of 0, 4, 8 and 16 barrels was tested by using the procedure in Section 4.6, and the step responses was measured at 1000 sec., 1600 sec., 1400 sec. and 1050 seconds respectively. The measurements was conducted at different times to avoid impeding the SPM during the procedure.

Although we refer to the gas kick volume here, the unit is of mass (metric tons) because of the formulation in (5.10). The results of the experiments can be found in Figure 5.6, and as can be seen there is a linear correlation in all the models.

5.3.5 Model from Rig pump to SPP

Finally, it is made a model from the rig pump to the stand pipe pressure (SPP) to make the controller able to prevent the mud level in the drill string from sinking, see Section 2.5 The model was estimated the same way as the model from the rig pump to the BHP, i.e by finding a correlation between the two and then derive the derivative to describe the gain. The resulting gain function can be seen below[1].

$$G_{rig}^{SPP} = 2 \cdot 4.276 \cdot 10^{-5} \cdot q_{rig} + 4.108 \cdot 10^{-3} \tag{5.11}$$

[1]Plots of the identification and gain can be found in Appendix B.

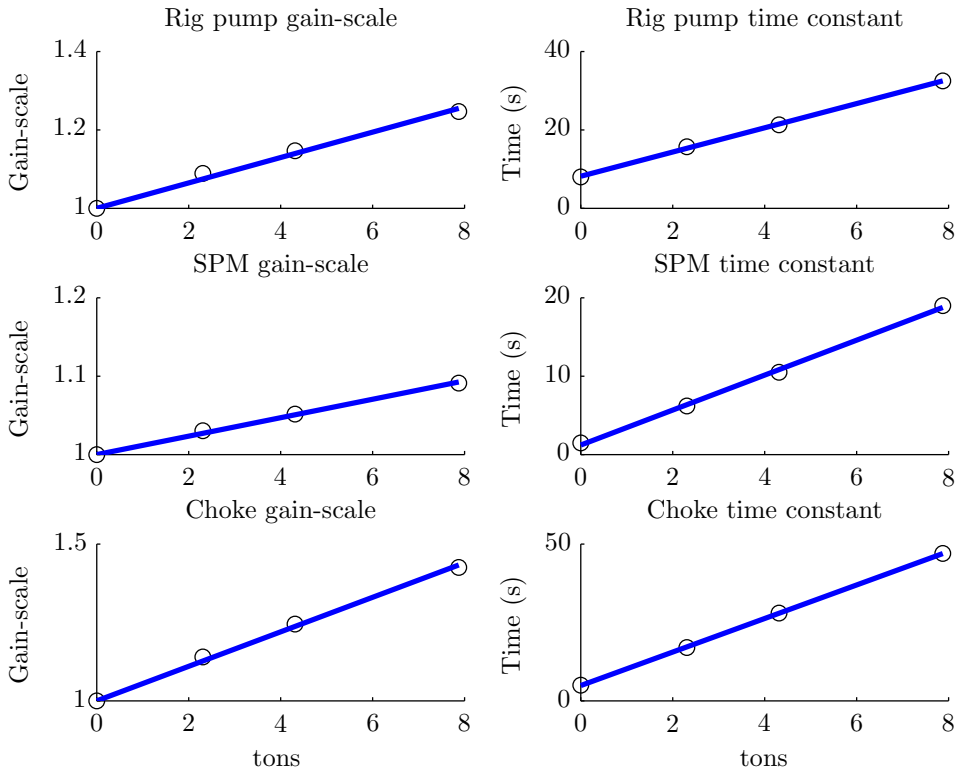

FIGURE 5.6: This figure shows how the time constants and gains vary with the kick size in equivalent tons of mud. Note that the gains is only a scaling of the original, i.e. they are 1 when the kick size is zero.

The time constant was found to be non-varying and equal to 4 seconds. Correction for the kick volume was deemed unnecessary as it doesn't directly affect the SPP, therefore such a model correction was not implemented.

5.4 Tuning

Tuning is in general done by choosing the weight matrices Q_y, Q_u and P from equation (3.2) in order to prioritize different states to each other. The most important states gets the highest weight. To make the weighting process easier each weighting element in the matrices consist of two parameters: $Span$ and $Fulf$, see equation (5.12). $Fulf$ can be thought of as the weighting parameter whereas $Span$ is meant to describe the accepted variation in the corresponding state.

$$Q[x] = \frac{Fulf}{Span} \tag{5.12}$$

where $Q[x]$ is an element on the diagonal.

By setting all the $Fulf$ parameters to 1 and setting the $Span$ parameters to the desired variation, the engineer has a good starting point when the $Fulf$ parameters is adjusted to acquire the right weighting.

The final tuning parameters that has been used in the simulations can be found in Table 5.2 and 5.1.

Table 5.1: Tuning parameters of the CVs

CV	Span	Set point	Fulf	Set point prio
BHP	1	142	1	10
	Span	Low limit	Low penalty	Low prio
SPP	2	3	1	1

Table 5.2: Tuning parameters of the MVs

MV	Span	IV	Fulf	IV prio	Move penalty
Rig pump	100	1000	1	60	2
SPM	100	None	None	None	5
Choke	5	100	1	70	0.5

It has not been implemented any hard constants on the CVs, but the hard constraints implemented on the MVs can be found in Table 5.3.

Table 5.3: Hard constraints of the MVs

MV-Hard	Max up	Max down	Low limit	High limit
Rig pump	20	-20	400	2000
SPM	150	-150	290	2000
Choke	10	-10	25	100

5.4.1 Blocking and prediction horizon

When looking at the time constants in Figure 5.6 it is evident that the time constants indeed vary with the size of the kick. A kick of 16 barrels, which is a quite big kick, will cause a maximum gas volume equivalent to 15 tons of mud.

The prediction horizon has therefore been set to 10 minutes gives a good margin even for larger kicks.

The blocking was chosen the same for all MVs:

$$\text{Blocking} = [2 \quad 4 \quad 7 \quad 11 \quad 16 \quad 22] \tag{5.13}$$

The CVs are not necessarily evaluated at the same time as the MVs, and in this case the evaluation points was located at:

$$\text{EvalPntBHP} = [2 \quad 6 \quad 13 \quad 24 \quad 35 \quad 40 \quad 70 \quad 105 \quad 140 \quad 171] \tag{5.14}$$

$$\text{EvalPntSPP} = [2 \quad 6 \quad 13 \quad 14 \quad 24 \quad 28 \quad 40 \quad 42 \quad 56 \quad 66] \tag{5.15}$$

Observe that the CVs does not have to be evaluated at the same time either.

Chapter 6

Simulation and Results

6.1 Connecting SEPTIC with Dymola

This section has been taken from the report written in the specialization project.

To connect Dymola and SEPTIC, Dymola's OPC server was used. The OPC protocol enables the clients to change the variables in the system in real-time. All synchronization is handled in the protocol and almost no configuration is required to get the server going. In SEPTIC a configuration file must be updated with the correct server name and schedule tag. In Dymola this server is called "Dymosim.OPCServer.1" and all variables, known as "tags" in OPC terminology, is available in the object, ModelVariables. By changing the tag "tScale" it is possible to speed up the simulation.

The computer used in this project was a Lenovo ThinkPad X201 with a Intel Core i5 M540 processor running at 2.53GHz. This computer managed a simulation speed of 20 times real-time, i.e., tScale was set to 0.05.

6.2 Pressure profiles

To get a better understanding of the system it can be useful to look at the pressure profiles in Figure 6.1. The profiles is taken from a simulation with a 4 barrel gas kick controlled with the PI controller. Notice that the gas in the SPM curves the profile upwards thus compensating the lack of SPM head.

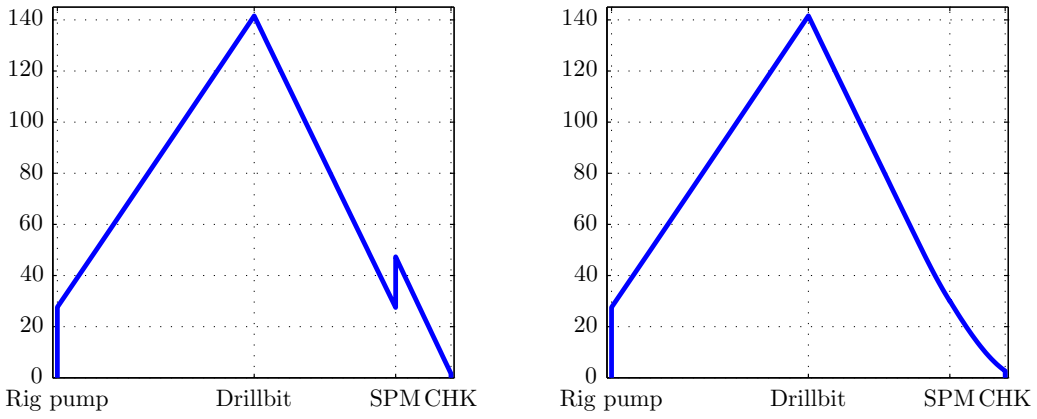

(a) Pressure profile at steady state

(b) Pressure profile with gas in SPM

FIGURE 6.1: Pressure profiles in bar with PI control

6.3 Simulation with 4 barrel gas kick

When the system is subjected to a 4 barrel kick both SEPTIC and the PI controller struggles to keep the BHP set point. The problems arises at very point where the SPM is in the transition from full head to total head loss. In this phase of the simulation it will be impossible to maintain the BHP at set point because the gas hasn't yet expanded sufficiently to lower the hydrostatic pressure and thus compensating the head loss.

As mentioned in the paragraph above, the increase in the BHP at 50 minutes in Figure 6.2, is due to head loss in the SPM. The controller sets the choke wide open to compensate, however, due to saturation it is impossible to control the pressure at this point.

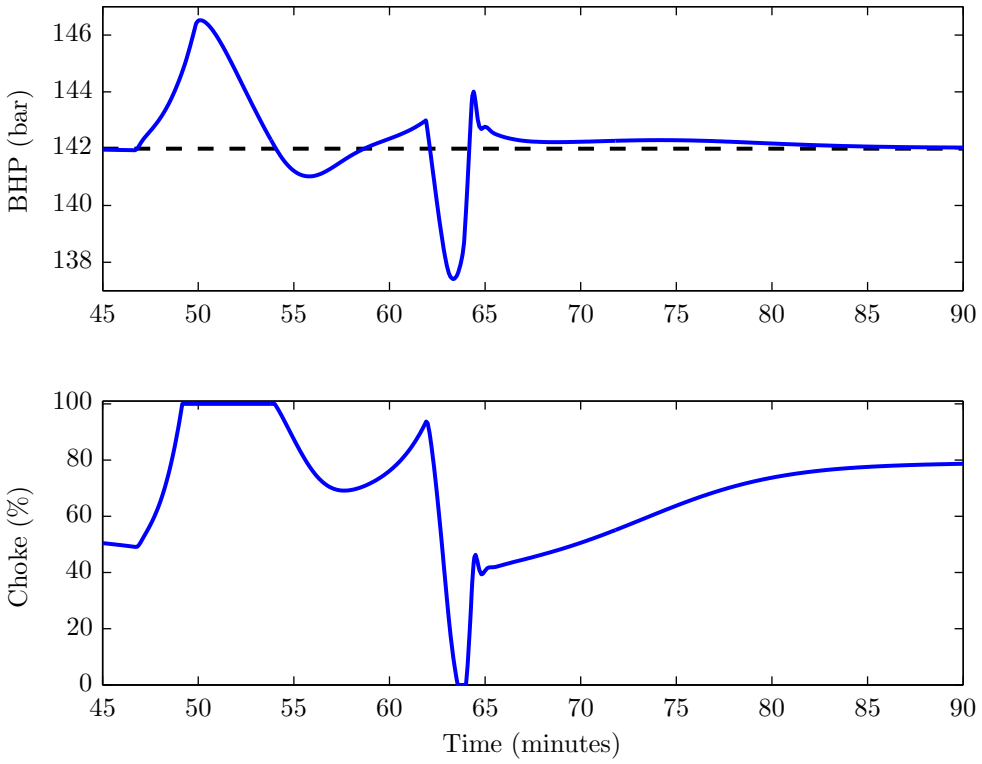

FIGURE 6.2: Simulation with 4 barrel gas kick controlled with the PI controller. The black dashed line is the set point.

When the simulation reaches 63 minutes the PI controller faces another major challenge. Around that time the gas fraction in the SPM drops rapidly from 20% down to 10% which causes a sudden head gain in the SPM. This pressure spike arises too fast for the controller to react in time hence the the large pressure drop at this time.

The head loss in the SPM poses problems for SEPTIC as well as can be observed in Figure 6.3 at about 50 minutes. Initially SEPTIC tries to use the SPM to compensate, but when the high threshold forces the rotational speed down and the head loss prevails, SEPTIC finally starts lowering the rig pump flow. At this point both the rig pump and the choke becomes saturated, i.e. the rig pump cannot go any lower because the SPP needs to be above 1 bar.

At about 63 minutes SEPTIC is steadily increasing the SPM, thus avoiding the pressure spike which caused problems for the PI controller In Figure 6.4 it shown

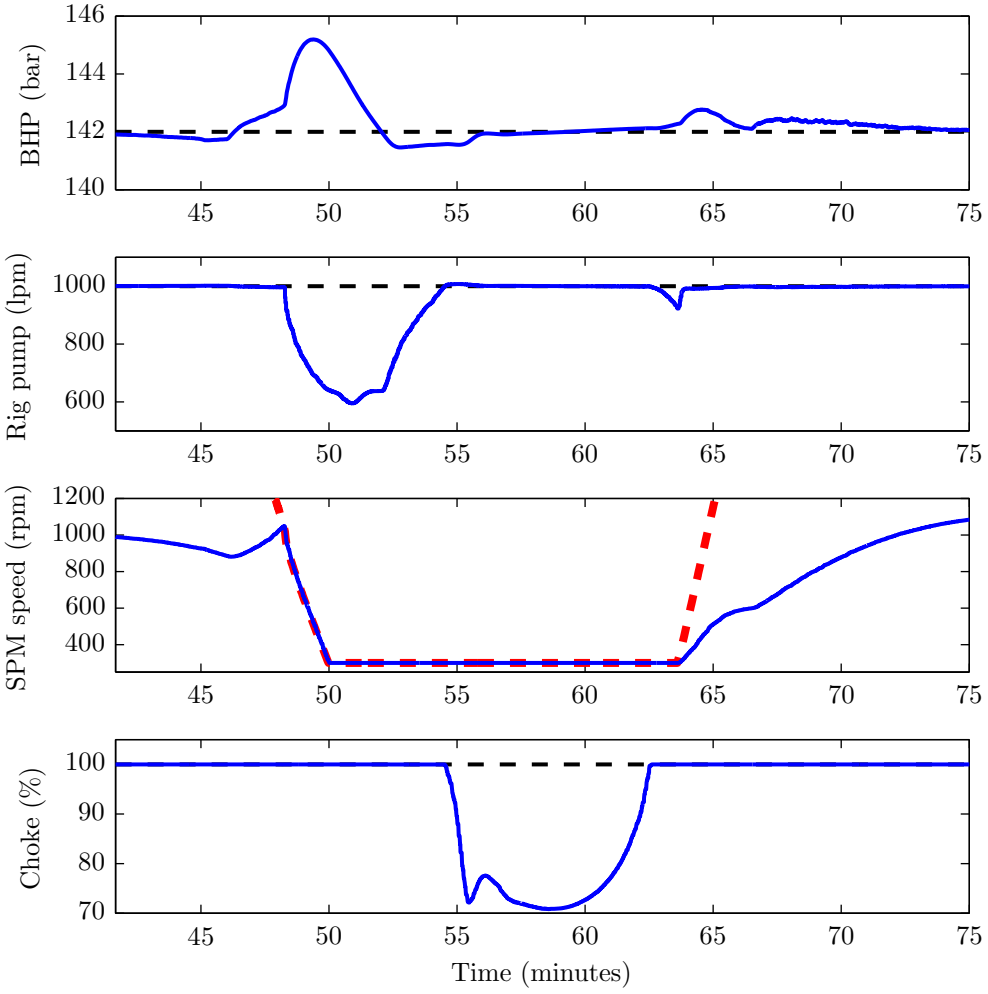

FIGURE 6.3: Simulation with 4 barrel gas kick controlled with SEPTIC. The black dashed line is the set point or IV, and the red dashed line is the varying threshold of the SPM.

a picture from SEPTIC's user interface when the PI controller encounters the first pressure increase seen in Figure 6.2. The red graph is the BHP measurement, red yellow graph shows the estimated steady state solution, and the green graph shows the relative model error.

The yellow curve lies on the set point at all times except around 12:35 where SEPTIC estimates that the pressure rise to 148 bar even when all control actions are taken into account. Shortly after SEPTIC realize that the solution actually lies

considerably lower and attributes the erroneous prediction to model error, hence the steep decent of the green curve.

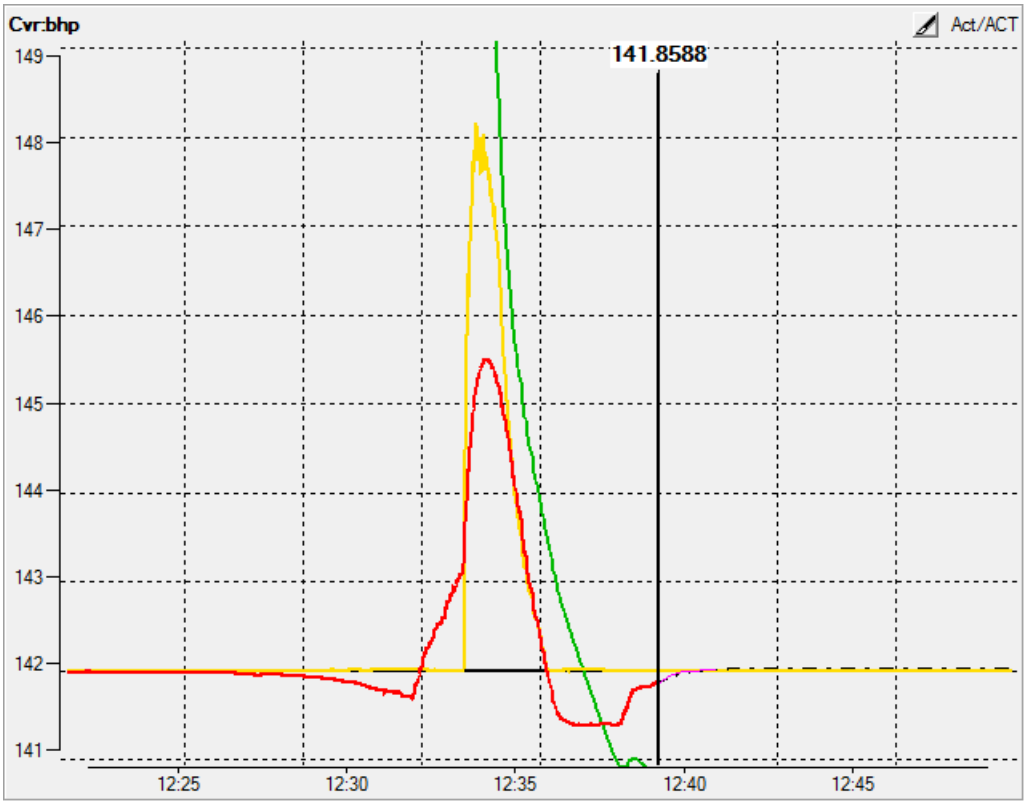

FIGURE 6.4: SEPTIC's estimation of steady state solution and model error. The picture is from SEPTIC's user interface.

In this simulation case it is evident that SEPTIC has an advantage over the PI controller. The largest deviation is reduced from just under 5 bar to just above 3 bar. In addition SEPTIC manages to keep the BHP closer at a general basis as well.

6.4 Simulation with 16 barrel gas kick

When the kick increases to 16 barrels the challenges is somewhat different. By the time the kick arrives the SPM, the gas volume has increased sufficiently to compensate for the SPM head loss. The kick has also been distributed on a larger area causing the the head loss to last for a larger period of time. However, despite

this increase in time, it seems that the gas fraction varies faster then for the 4 barrel kick.

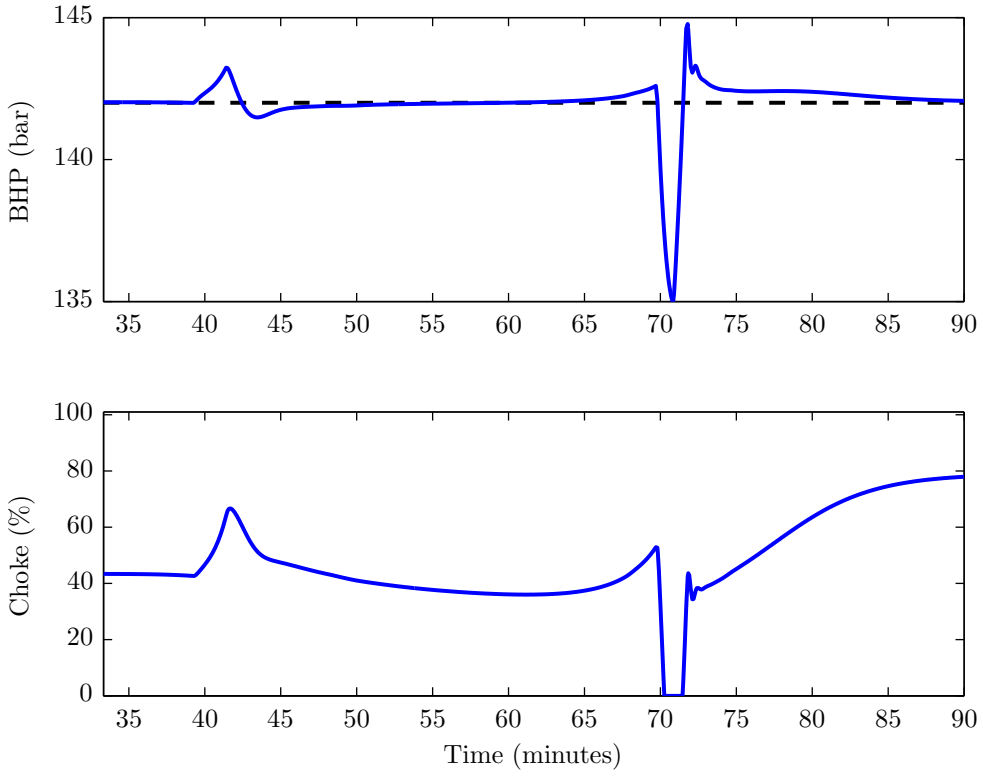

FIGURE 6.5: Simulation with 16 barrel gas kick controlled with the PI controller. The black dashed line is the set point.

The PI controller encounters less problems in this simulation case, see Figure 6.5. At 42 minutes when the SPM is impeded, the PI controller manages to keep the BHP at just above 143 bar before getting it back down. During the period up to the gas exit, the controller manages to keep the set point more or less al the way. As the gas exits and the SPM regain its head, a pressure drop of 7 bar occurs for the same reasons as with the smaller kick. However, the previous simulation only experienced a drop of just below 5 bar thus the PI controlled system performs worse as the kick size increases.

Notice also that the choke opening is kept much smaller through this simulation case. This is due to the lower hydrostatic pressure which forces the controller to throttle the choke to compensate.

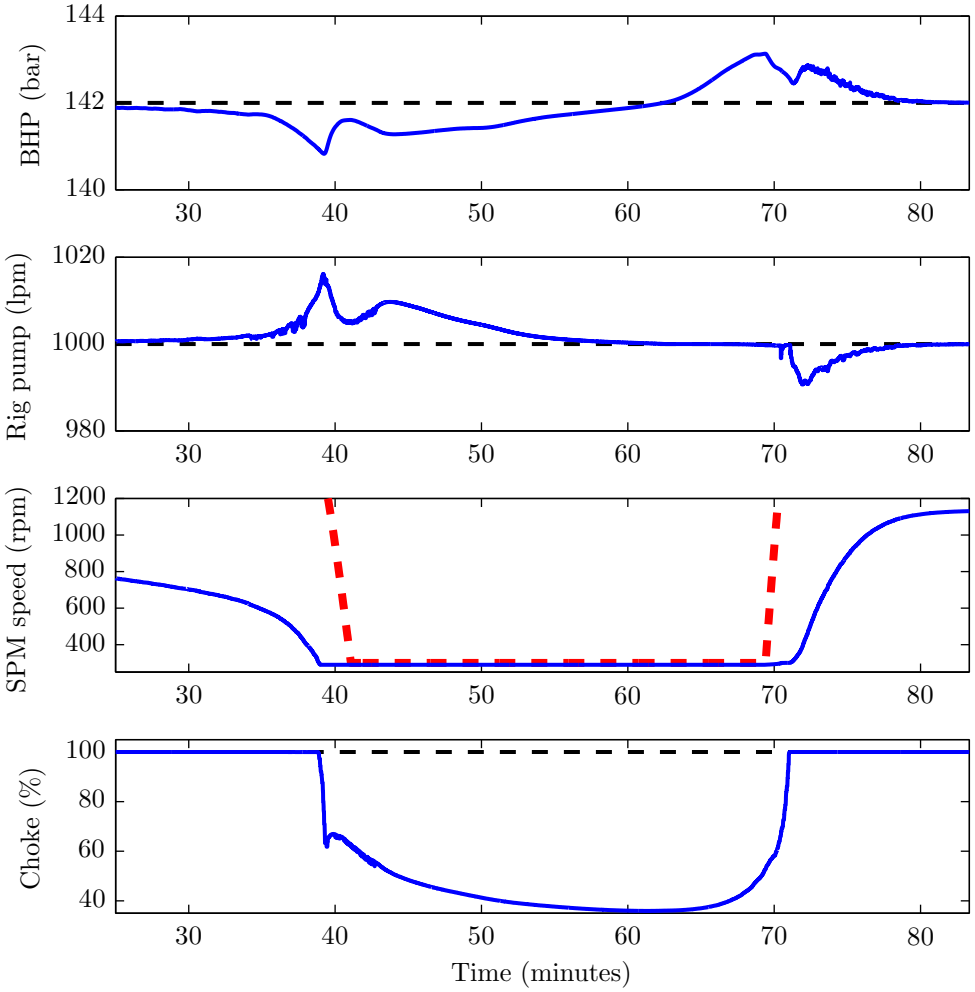

FIGURE 6.6: Simulation with 16 barrel gas kick controlled with SEPTIC. The black dashed line is the set point or IV, and the red dashed line is the varying threshold of the SPM.

As for the PI controller, SEPTIC also avoids saturation when gas arrives at the SPM, however, there are some interesting observations to be made. Whereas the PI controller keeps the choke opening about 50% in this phase, the SEPTIC keeps the choke wide open trying to cope with the pressure loss by increasing the flow and lowering the SPM. Notice that the red high threshold is not binding in this simulation. Only when the SPM is saturated SEPTIC begins to throttle the choke. Despite all these control actions the PI controller actually keeps better track of the BHP in the middle section.

When the gas is exiting SEPTIC is again the best controller keeping the BHP just above 143 bar at the worst peak. The PI controller in comparison experience deviations to 135 bar and 145 bar in just 2 minutes time.

6.5 Simulation with 32 barrel gas kick

In the final simulation the kick has been increased to 32 barrels of gas measured at 142 bar. This is a very large kick which is illustrated by a gas fraction in the SPM that peaks at 78.4%. In comparison, the 4 barrel kick causes the gas fraction in the SPM to peak at only 30.4%.

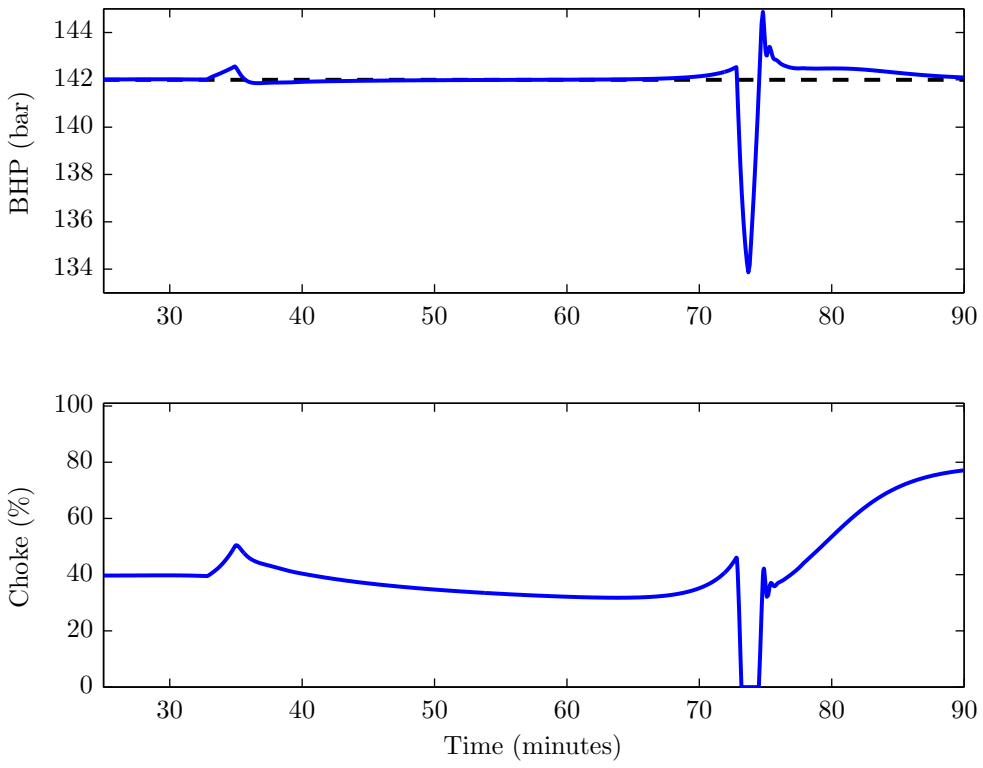

FIGURE 6.7: Simulation with 32 barrel gas kick controlled with the PI controller. The black dashed line is the set point.

Once again there is a slight improvement for the PI controller as gas enters the SPM, relative to the smaller kicks. As can be seen in Figure 6.7 the BHP deviates about 0.5 bar with only a minor response in the choke opening. This deviation

could possibly be smaller as the PI controller was only tuned for the 4 barrel kick. As the gas exits the SPM the pressure drops rapidly just like for the other PI controlled simulations. This time it drops below 134 bar causing an 8 bar deviation.

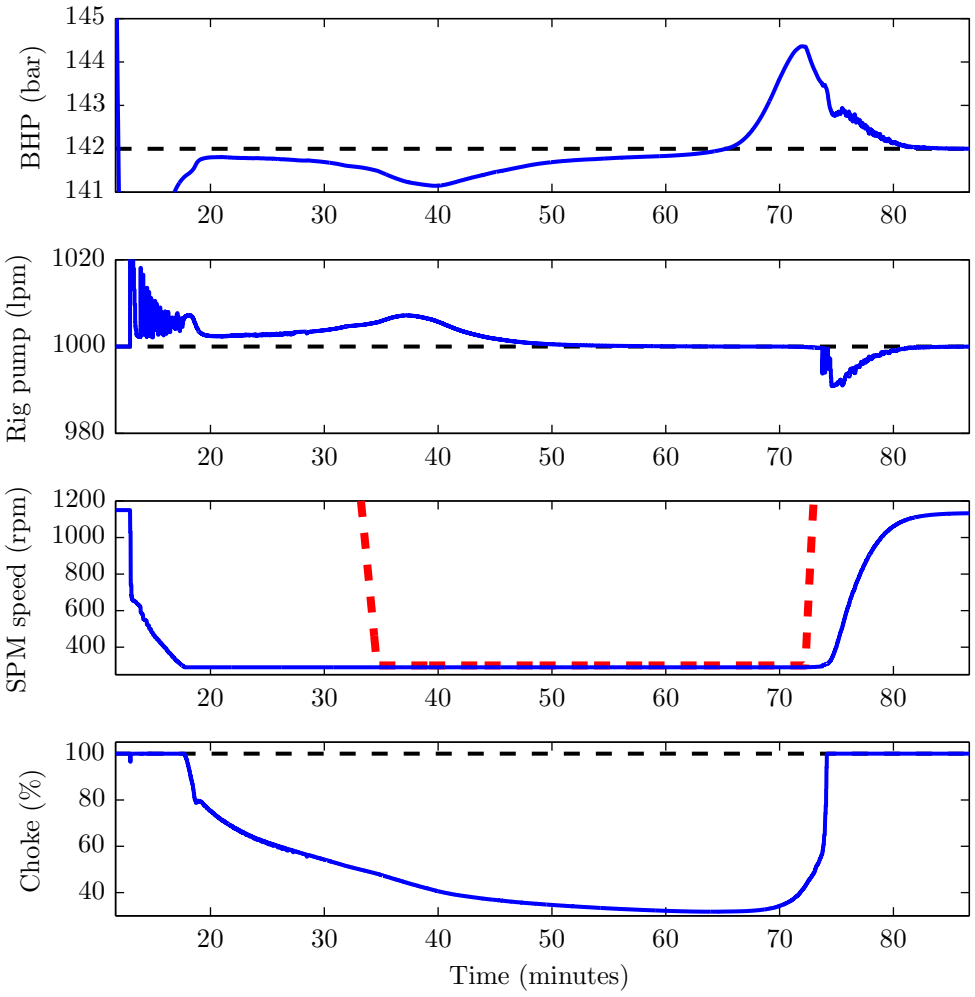

FIGURE 6.8: Simulation with 32 barrel gas kick controlled with SEPTIC. The black dashed line is the set point or IV, and the red dashed line is the varying threshold of the SPM.

In the corresponding simulation with SEPTIC the BHP deviation is approaching 2.5 bar at the worst peak, see Figure 6.8. Transients due to the kick emulation last until 20 minutes, thus it is only worth considering the behaviour after this point. When the gas hits the SPM the deviation approaches 1 bar which is worse

than the PI controller. At 70 minutes SEPTIC seems to overestimate the head of the SPM causing a substantial deviation of 2.5 resulting in a BHP of 144.5.

As 2.5 bar is deemed as the highest allowable deviation when utilizing a model predictive controller, it is evident that 32 barrel kick is the largest that SEPTIC in the current configuration can handle. An exception from this criteria is made in the first simulation as the system was saturated in the critical period.

Chapter 7

Discussion

The results in Chapter 6 shows that the MPC is capable of ventilating out larger gas kicks than a simple PI controller. In fact, the MPC managed to perform better in all simulation cases, spanning from 4 to 32 barrel kicks.

In Section 6.3 a 4 barrel kick is simulated. Both the MPC and the PI controller handles the pressure increase at the beginning satisfactory in the sense that they saturate the MVs, which means that no better solution exists. However, because the MPC can lower the rig pump flow it is able to keep the BHP roughly 25% closer to the set point. As the simulations progresses forward it can be observed that the MPC outperforms the PI controller until about 62 minutes. Whereas the PI controller vary about 1 bar of deviation, the MPC lies around 0.5 bar. After 62 minutes of simulation the MPC beats the PI controller an error of just under 1 bar whereas the PI controller gets an error of 4 bar. The reason for that large deviation in the PI controlled system is that, unlike with the MPC, the SPM is not brought down to idle speed while impeded. It operates at 1150 rpm throughout the simulation creating problems when the gas is about to exit.

Figure 6.4 shows that the SEPTIC is attributing the erroneous prediction to model error. This is perhaps the most important source to bad performance in the two last simulations because the estimated model error is incorporated in the model used to predicate the future. The erroneous prediction is obviously due to the

non-modelled disturbance from the gas kick, thus the models might still be valid although they probably has some imperfections.

The simulations in Section 6.4 deals with a gas kick of 16 barrels which changes the challenges a bit from those faced in Section 6.3. The saturation problem is no longer an issue and both controllers manages a deviation of only 1 bar in the first phase. However, they are not maintaining the set point perfectly. The PI controller tries to take measures in order to bring the BHP back to the set point, but it fails to open the choke sufficiently.

The MPC on the other hand, struggles to keep to BHP high enough. It attempts accommodate the issue by adjusting the SPM speed and to some extent the rig pump flow, but non-modelled disturbance makes SEPTIC assume that the control actions taken ought to suffice. Due to this fact SEPTIC has almost no benefit from its calculated predictions as it is forced to move in the opposite direction of what it predicated in the time instant before.

At the point of gas exit it can be observed in Figure 6.6 that the SPM should have been increased faster to lower the BHP deviation. It does albeit try accomodate the issue by opening the choke, but it is evidently not sufficient. This could perhaps be improved by some further tuning, however, it is more likely to be caused by model errors.

The last simulation found in Section 6.5 addresses the 32 barrel kick. The qualitative observations in these simulations are the same as in the 16 barrel case. The MPC struggles with unmeasured disturbances and lies about 0.5 bar from the set point in average before the pressure peak at 72 minutes.

7.1 Suggested improvements

The linear MPC with dynamic models[1] is undoubtedly a good improvement over the PI controller, however, it is not flawless in its current state. The main obstacle

[1] A simulation with static models can be found in Appendix A

seems to be the lack of disturbance models which would make the controller able to take more appropriate actions during control.

Another solution, which has been considered to be included in this thesis, is the possibility to replace the centrifugal pump with a positive displacement pump in the SPM. Some simulations with a idealized displacement pump has shown promising results and it might be worth considering if the performance needs to increased. However, to authors knowledge, positive displacement pumps are in general difficult to utilize in drilling systems like the one investigated here. I might therefore be infeasible in terms of implementation costs.

Chapter 8

Conclusion

It has been shown that a linear model predictive controller with dynamic models is able to outperform a simple PI controller with respect to maximum deviation during gas ventilation. Furthermore, it has been shown that the MPC is able to handle as much as a 32 barrel kick while keeping the BHP within a margin of ± 2.5 bar. The MPC has, nevertheless, shown some weaknesses, especially when the disturbance changes fast because the algorithm attributes the prediction error the models when it in fact is a non-modelled disturbance.

Further research could focus on developing a disturbance model with the kick volume as the disturbance variable. Another improvement could be the use of a positive displacement pump since this will not be impeded by the gas thus avoiding many problems. It could also be worth investigating whether a nonlinear MPC could improve the performance over the linear MPC.

Finally it would be preferred to find another way spin down the SPM than using a multiphase meter.

Appendix A

Simulation with static models

These simulations has been taken from the report written in the preceding specialization project.

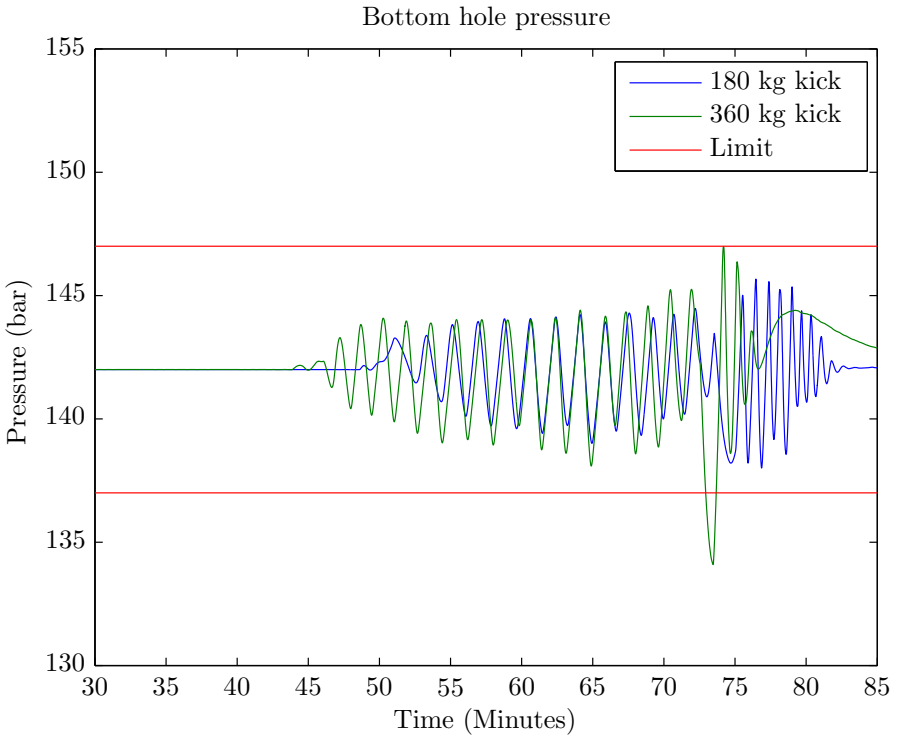

FIGURE A.1: This plot shows violent oscillations due to model error. MVs are the rig pump and the choke. The gas kick corresponds to 7 and 14 barrels of gas.

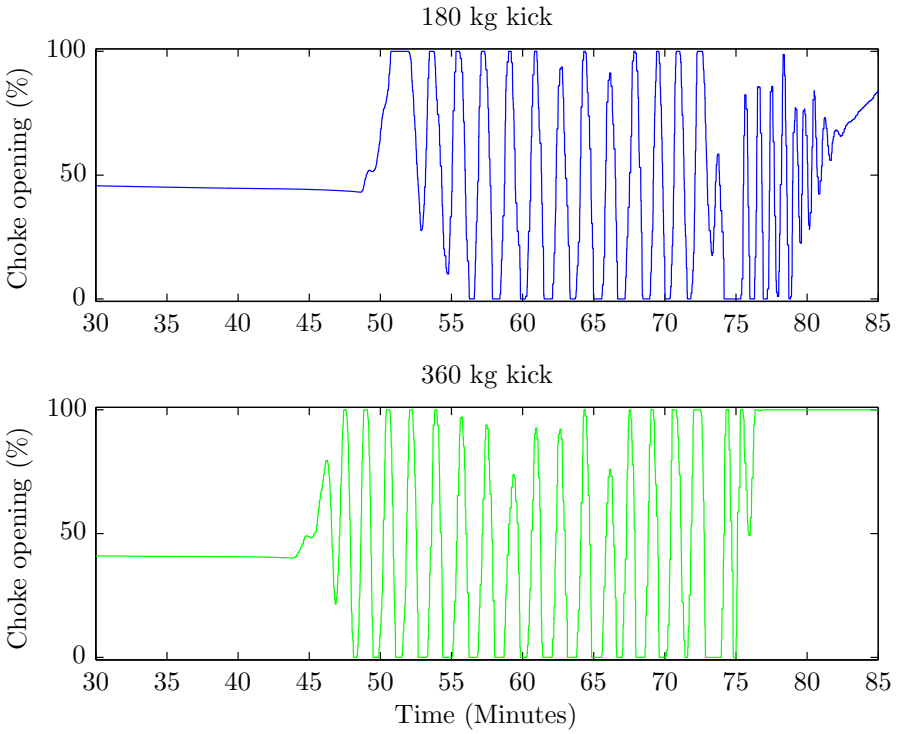

FIGURE A.2: This plot shows how the choke is oscillating due to both incorrect gain and time constant.

Appendix B

Identification of rig pump to SPP model

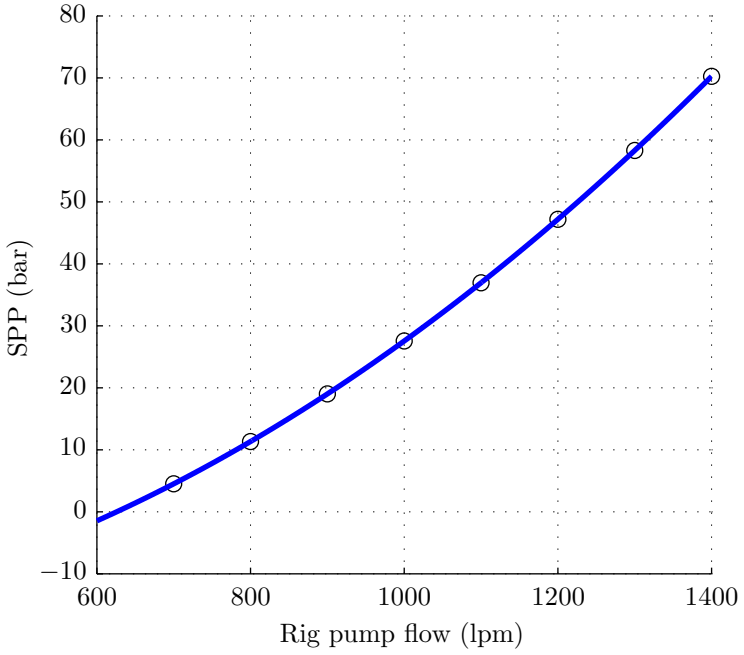

FIGURE B.1: The plot shows how the SPP varies with rig pump flow. The black circles are the measured date and the blue line is the estimated function.

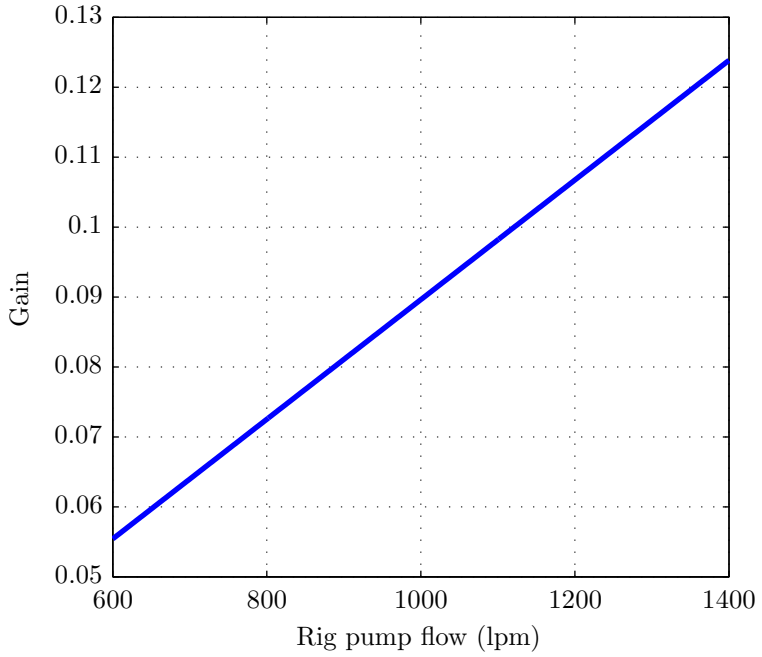

FIGURE B.2: The plot shows the gain from the rig pump to the SPP

Bibliography

[1] D. Hannegan. Case studies-offshore managed pressure drilling. *Proceedings for SPE Annual Technical Conference and Exhibition*, (SPE 101855), September 2006.

[2] Gerhard Nygaard Øyvind Breyholtz and Michael Nikolaou. Automatic control of managed pressure drilling. *American Control Conference*, 21:442–447, July 2010.

[3] H. Asheim. Subsurface equipment/artificial lift: Maximizing production from the well. *Society of Petroleum Engineers*, (SPE 56659), October 1999.

[4] M.M. Awad. Chapter 11 – two-phase flow. October 2012. doi: 10.5772/54291. URL `http://www.intechopen.com/books/export/citation/BibTex/an-overview-of-heat-transfer-phenomena/two-phase-flow`.

[5] Frank M. White. *Fluid Mechanics*. McGraw-Hill, 6 edition, 2009.

[6] Erlend Mjaavatten Øyvind Nistad Stamnes and Kristin Falk. A simplified model for multi-fluid dual gradient drilling operations. *Proceedings of the 2012 IFAC Workshop on Automatic Control in Offshore Oil and Gas Production*, pages 211–216, June 2012.

[7] O. M. Aamo G.-O. Kaasa, Ø. N. Stamnes and L. S. Imsland. Simplified hydraulics model used for intelligent estimation of downhole pressure for a managed-pressure-drilling control system. *Society of Petroleum Engineers*, pages 127–138, March 2012. doi: doi:10.2118/143097-PA. URL `https://www.onepetro.org/journal-paper/SPE-143097-PA`.

[8] John-Morten Godhavn Øyvind Breyholtz Jing Zhou, Gerhard Nygaard and Erlend H. Vefring. Adaptive observer for kick detection and switched control for bottomhole pressure regulation and kick attenuation during managed pressure drilling. *American Control Conference*, pages 3765–3770, July 2010.

[9] Ahmed M. Al-Naamany Ali Al-Bimani Khamis Al-Busaidi Mahmoud Meribout, Nabeel Z. Al-Rawahi and Adel Meribout. A multisensor intelligent device for real-time multiphase flow metering in oil fields. *IEEE Transactions on Instrumentation and Measurement*, 59(6):1507–1519, June 2010.

[10] Jorge Nocedal and Stphen J. Wright. *Numerical Optimization*. Springer Verlag, 2 edition, 2006.

[11] Stig Strand and Jan Richard Sagli. Mpc in statoil – advantages with in-house technology. *Statoil Research and Development, Process Control*, 2003.

[12] Bjarne Foss and Tor Aksel N. Heirung. Merging optimization and control. September 2013.

[13] Jan Marian Maciejowski. *Predictive Control with Constraints*. Prentice Hall, 1 edition, 2002.

[14] C.F. Colebrook. Turbulent flow in pipes, with particular reference to the transition region between the smooth and rough pipe laws. *Journal of the Institution of Civil Engineers*, 11(4):133–156, May 1939.

[15] *Control Valve Handbook*. Emerson Process Management, 4 edition, 2005. URL `http://www.documentation.emersonprocess.com/groups/public/documents/book/cvh99.pdf`.